THESIS-2022

The 5th symposium on two-phase modeling for sediment dynamics in geophysical flows

June 6-10, 2022

Les Houches School of Physics, France

Book of abstracts

Organizing committee

Julien CHAUCHAT, Univ. Grenoble Alpes, CNRS, Grenoble INP, LEGI, Grenoble, France

David HURTHER, Univ. Grenoble Alpes, CNRS, Grenoble INP, LEGI, Grenoble, France

Philippe FREY, Univ. Grenoble Alpes, INRAE, UR ETNA

Nico Gray

Coupling rheology and segregation in granular flows

During the last fifteen years there has been a paradigm shift in the continuum modelling of granular materials; most notably with the development of rheological models, such as the μ(I)-rheology, but also with significant advances in theories for particle segregation. This talk details theoretical and numerical frameworks which unify these disconnected endeavours. The approach is based on the partially regularized incompressible μ(I)-rheology, which is coupled to the gravity-driven segregation theory of Gray & Ancey (J. Fluid Mech., vol. 678, 2011, pp. 353–588). The segregation and diffusion rates are based on the latest refractive-index matched shear box experiments, which show that the segregation rates are dependent of the local species concentration, the shear-rate, the pressure, the grain size and the grain-size ratio. The resulting advection–diffusion–segregation equations describe the evolving concentrations of the constituents, which then couple back to the variable viscosity in the incompressible Navier–Stokes equations. The numerical method is extensively tested in one-way coupled computations, before the fully coupled model is compared with the discrete element method simulations of Tripathi & Khakhar (Phys. Fluids, vol. 23, 2011, 113302) and used to compute the petal-like segregation pattern that spontaneously develops in a square rotating drum.

T. Barker, M. Rauter, E. S. F. Maguire, C. G. Johnson & J. M. N. T. Gray (2021) Coupling rheology and segregation in granular flows. J. Fluid Mech. 909, A22.

T. Trewhela, C. Ancey & J. M. N. T. Gray (2021) An experimental scaling law for particle-size segregation in dense granular flows. J. Fluid Mech. 916, A55.

How diffusion of momentum and sediment keeps rivers close to the threshold of transport

Eric Lajeunesse, O. Devauchelle, F. Métivier
P. Popović, A. Abramian

Alluvial rivers build their channel in a bed of mobile sediment, such as sand or gravel. The feedback between the flow of water and the mechanics of sediment transport thus selects the shape and size of rivers, in a way that is not fully understood yet[6]. Field observations show that rivers adjust their shape so that the sediment that makes up their bed is close to the threshold of entrainment[5,7,8]. Below this threshold, a river deposits all the sediment it carries, and its bed builds up until it eventually reaches the threshold. Conversely, above the threshold, erosion of the bed quickly brings the river back to the threshold. Based on this simplistic reasoning, early theories assumed that rivers construct their own bed so that sediments are exactly at the threshold of motion[2,3,10]. This so-called "threshold theory" accounts for the observation that the width of rivers increases as the square root of their discharge, an empirical relation known as Lacey's law[4]. Yet, the shape of alluvial rivers is highly sensitive to sediment transport : even a small departure from threshold induces a significant change in the channel's shape. Since sediment transport is difficult to measure in the field, we investigate its influence in small laboratory rivers, in which a laminar flow erodes a layer of plastic grains[1]. We show how the diffusion of the momentum carried by the flow combines with gravity and the diffusion of traveling grains to determine the shape of a river[9]. This model reliably reproduces the experiments without any tuning, and confirms the hypothesis, originally proposed by Parker[6], that rivers only form close to the threshold of sediment motion. Although our results relate directly to experimental, laminar rivers, they likely apply qualitatively to natural ones, potentially allowing us to use the shape of a river as a proxy for its sediment discharge.

RÉFÉRENCES

[1]Abramian, A, Devauchelle, O, & Lajeunesse, E. 2020. Laboratory rivers adjust their shape to sediment transport. *Physical Review E*, **102**(5), 053101.

[2]Glover, R. E., & Florey, Q. L. 1951. Stable channel profiles. *U. S. Bur. Reclamation, Hydr. 325.*

[3]Henderson, F. M. 1961. Stability of alluvial channels. *J. Hydraul. Div. ASCE*, **87**, 109–138.

[4]Lacey, G. 1930. *Stable channels in alluvium.*

[5]Métivier, François, Lajeunesse, Eric, & Devauchelle, Olivier. 2017. Laboratory rivers : Lacey's law, threshold theory, and channel stability. *Earth Surface Dynamics*, **5**(1), 187.

[6]Parker, G. 1978. Self-formed straight rivers with equilibrium banks and mobile bed. Part 2. The gravel river. *J. Fluid Mech.*, **89**, 127–146.

[7]Phillips, Colin, Masteller, Claire, Slater, Louise, Dunne, Kieran, Francalanci, Simona, Lanzoni, Stefano,

Merritts, Dorothy, Lajeunesse, Eric, & Jerolmack, Douglas J. In press. The importance of threshold in alluvial river channel geometry and dynamics. *Nature Reviews Earth & Environment*.

[8]Phillips, Colin B, & Jerolmack, Douglas J. 2016. Self-organization of river channels as a critical filter on climate signals. *Science*, **352**(6286), 694–697.

[9]Popović, Predrag, Devauchelle, Olivier, Abramian, Anaïs, & Lajeunesse, Eric. 2021. Sediment load determines the shape of rivers. *Proceedings of the National Academy of Sciences*, **118**(49).

[10]Seizilles, G., Devauchelle, O, Lajeunesse, E., & Métivier, F. 2013. Width of laminar laboratory rivers. *Phys. Rev. E.*, **87**, 052204.

Olivier Pouliquen

Continumm description of granular flows: dry, wet, and cohesive grains…

Knowing the rheology of granular media under steady and uniform shear is the first step towards the development of an hydrodynamics approach of granular flows. In this talk, I will review our knowledge of the rheology of dense granular media in different conditions: for dry granular media (grains in air), for viscous suspensions (grains in a viscous liquid), for the intermediate regime where the viscous/inertial transition occurs. The case of cohesive materials when adhesive forces exist between the grains will also be discussed. In a second part I will illustrate how the knowledge of the constitutive laws in the steady uniform regime might not be sufficient to describe more complex flows when transient features or strong heterogeneities are present.

Title: Using Unmanned Survey Vehicles to Measure Coastal Morphodynamic Processes

Author: Peter Traykovski, Applied Ocean Physics and Engineering Department, Woods Hole Oceanographic Institution

In the past decade our ability to model complex two-phase systems with sediment and water such as rivers, estuaries, and coastal oceans have increased dramatically, but measurement methods to evaluate the performance of these models are expensive, time consuming and difficult to use. In systems with intermittent water coverage, during storms, floods or high tides or robotic aerial platforms (e.g. drones) have revolutionized our ability to take accurate high resolution measurements at the event time scale. While autonomous underwater vehicles have found widespread use in deeper water, in very shallow water (less than 5 m) where morphodynamic processes are most active, vehicles at the surface are preferrable to an underwater vehicles due to GPS loss underwater and the increased swath of bathymetric sensors with increased distance from the seafloor.

This talk will highlight recent development of unmanned surface vehicles (USVs) that can be launched by one or two people, are capable of operating in rough surf zone conditions or flooding rivers and have very simple user interfaces similar to an aerial drone. The goal of this work is to develop “drones of the oceans” that can measure nearshore morphological change in a similar manner to aerial drones. The talk will also highlight two sets of results from these systems that illustrate challenges in multiple scale problems that are revealed by the measurements. In one set of measurements, USVs combined with aerial drones were used to measure bedform resolving bathymetry, tidal flow, and tidal water surface elevation in a tidal estuary. This allows estimation of drag coefficients and comparing models for flow and friction over bedforms with observations. In the seconds set of observations USVs were used to make repetitive measurements of ocean facing beach and sand bar morphology on both the seasonal and storm event time scale. Some of these surveys also resolved smaller scale bedforms on superimposed on the sandbars suggesting that multiple scale approaches maybe be required for modelling sand bar dynamics.

Investigating sediment dynamics with the aid of particle-resolved direct numerical simulation

Markus Uhlmann
Institute for Hydromechanics
Karlsruhe Institute of Technology

The motion of sediment particles in many geophysical systems is driven by a turbulent flow. Depending on the parameter values a variety of transport modes can be observed, including the formation of sediment patterns with different geometries and length-scales. These patterns, in turn, may have a substantial effect on the overall flow properties and upon the transport rates of the grains themselves. Over the past decade, the approach of numerically simulating the motion of individual grains while faithfully resolving all relevant scales of fluid motion has emerged as a powerful complement to laboratory experiments. While this technique is computationally quite intensive, it is able to provide spatio-temporally resolved data which is difficult to obtain by other means.

In the present contribution we will give an overview of the PR-DNS approach to turbulent sediment transport. We will cover algorithmic aspects which are key in providing the efficiency needed to tackle systems with large particle counts. We will discuss the need to conduct benchmarking tests versus well-established reference data-sets in order to establish the resolution requirements for a given method and a given configuration. We will then turn to results obtained in uni-directional open channel flow, where we observe transverse ripple patterns as well as streamwise-aligned ridge patterns. We will discuss the strategy of the 'minimal pattern unit' (inspired by the minimal flow unit of [1]) which can be employed in order to numerically establish a lower bound on the unstable pattern wavelength. A phase-averaging analysis of the flow field over a propagating ripple allows us to determine the profile of the basal shear-stress in relation to the contour of the pattern, and to put it into relation to the local sediment flux. Additional simulations of the flow over a smoothed ripple and over a stationary ripple allow us to determine the effects of porosity, roughness and mobility of the patterns upon the flow. Regarding ridge-shaped patterns, we have conducted an investigation of causality, showing that these patterns arise due to the eroding action of large-scale motions in the bulk of the boundary layer. We will also discuss the effect of sediment patterns on secondary flow, both in the presence and in the absence of bounding side-walls. Finally, we will present our results on the transport of contaminant particles in open channel flow over a sediment bed with and without patterns.

[1] J. Jimenez and P. Moin. "The minimal flow unit in near-wall turbulence." J. Fluid Mech. 225:213-240. 1991.

A study on vertical sorting mechanism in gravel bed rivers with graded sediment using the APM method

Takatoshi ATSUMI, Graduate Student of Science and engineering, Chuo University, Japan.
Email: a14.c3y6@g.chuo-u.ac.jp
Shoji FUKUOKA, Professor, Research and Development Initiative, Chuo University, Japan.
Email: sfuku@tamacc.chuo-u.ac.jp

Keyword: *gravel-bed rivers, sediment transport, vertical sorting, resolved CFD-DEM*

Abstract:

The bed material in gravel-bed rivers is composed of particles of various shapes and sizes. Various factors such as particle arrangement, porosity and particle collisions affect bed variation of gravel rivers in a complicated manner. In this study, we focused on the influence of the particle size distribution and conducted a numerical movable bed experiment with a mixed particle size using sphere in order to better understand the mechanism of gravel bed variation.

The numerical channel is straight with a channel length of 4.0 m and a width of 1.0 m. The particle size distribution is set with reference to the Talbot type and particle size has a spread of about 1 order (d=1.5~15cm). Numerical experiment was carried out under hydraulic conditions in which the largest particles of the bed surface moved. The numerical simulation model of Fukuoka et al. [1] is used. This model is a resolved CFD-DEM coupling method that can simulate three-dimensional motions of flows and gravel particles in different shapes and sizes.

After the water flowed for 50s, a clear vertical sorting was observed in the riverbed surface layer and on equilibrium was reached (Figure 1). The vertical distribution of Entrainment and Deposition, the right-hand side terms of the continuity equation $1/(1-\lambda)dz_b/dt = \sum D_k - \sum E_k$, was analyzed. Figure 2 shows the vertical distribution of Entrainment and Deposition for smallest(d=1.5cm) and the largest(d=15cm) particle size.

The analysis of E and D was carried out in the whole area of the channel. The analysis area was divided into layers of 5 cm in the vertical direction from the bottom of the channel. Every 10 s, the particles in each layer were judged to be detached (particle velocity is 5 cm/s or more) or deposited (particle velocity is 5 cm/s less), and E and D were calculated. In Figure 2(a), the smallest particles in the higher position of the surface layer are detached and deposited at a lower position around z=0.175m. On the other hand, at t=20-30s, many of the largest particles in the large particle population (z=0.225 m) buried in the bed surface layer were detached and deposited near the mean bed elevation. Large particles buried in the surface layer were exposed and detached mainly by interparticle collisions. In particular, at t=40-50s, which is close to the equilibrium state, the vertical distributions of E and D tend to coincide with each other for both the smallest and largest particle sizes. The difference in the vertical distribution of entrainment and deposition causes a change in the particle arrangement, indicating that it is important to consider these vertical distribution in the formation mechanism of vertical sorting.

Reference:[1]Fukuoka S., Fukuda T. and Uchida T., *Advances in Water Resources, Vol.72, pp.45-56*, 2014.

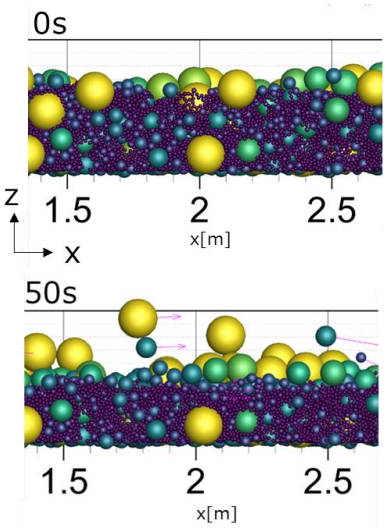

Fig.1 Time change of riverbed structure

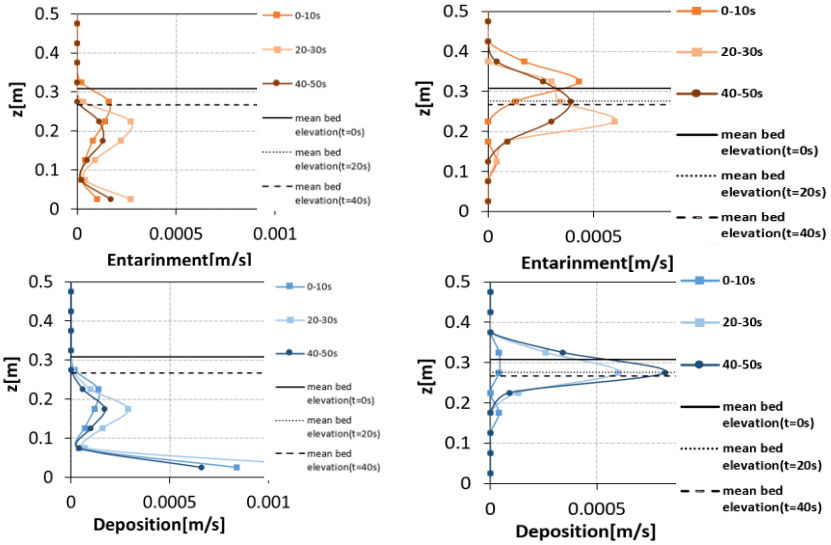

(a)d=1.5cm (b)d=15cm

Fig.2 Vertical distribution of Entrainmen and Deposition

Particle saltation over rigid, bumpy beds in viscous shearing flows

Diego Berzi[1] and Alexandre Valance[2]

[1]Department of Civil and Environmental Engineering, Politecnico di Milano, 20133 Milano,Italy

[2]Institut de Physique de Rennes, Universit´e de Rennes 1, Campus Beaulieu, 35 042 RennesCedex, France

We investigate the steady motion of solid particles through successive jumps over a horizontal, rigid, bumpy bed driven by the shearing of a viscous fluid in the absence of turbulence, lubrication forces and collisions above the bed. We employ a discrete element method for the particles coupled to a mean field continuum model for the fluid to run 2D simulations that we compare with the predictions of a simple model which assumes that all the particles follow identical, periodic trajectories determined by the intensity of the shearing and compatible with previously suggested laws relating the particle velocities before and after the impact with the bed. We solve the periodic model both numerically and analytically, and identify the solutions that are linearly stable to small perturbations. We show that the stable solutions of the periodic model are in qualitative and quantitative agreement with the discrete simulations, as long as the number of moving particles in the system is not too large. The discrete simulations further reveal that there are two distinct families of particle trajectories, and that the simple periodic model is actually a good representation of the more energetic particles, that spend most of their time in the upper flow layers where they can gain momentum from the flow.

Particle saltation over rigid, bumpy beds in viscous shearing flows

Diego Berzi[1] and Alexandre Valance[2]

[1]Department of Civil and Environmental Engineering, Politecnico di Milano, 20133 Milano,Italy

[2]Institut de Physique de Rennes, Universit´e de Rennes 1, Campus Beaulieu, 35 042 RennesCedex, France

We investigate the steady motion of solid particles through successive jumps over a horizontal, rigid, bumpy bed driven by the shearing of a viscous fluid in the absence of turbulence, lubrication forces and collisions above the bed. We employ a discrete element method for the particles coupled to a mean field continuum model for the fluid to run 2D simulations that we compare with the predictions of a simple model which assumes that all the particles follow identical, periodic trajectories determined by the intensity of the shearing and compatible with previously suggested laws relating the particle velocities before and after the impact with the bed. We solve the periodic model both numerically and analytically, and identify the solutions that are linearly stable to small perturbations. We show that the stable solutions of the periodic model are in qualitative and quantitative agreement with the discrete simulations, as long as the number of moving particles in the system is not too large. The discrete simulations further reveal that there are two distinct families of particle trajectories, and that the simple periodic model is actually a good representation of the more energetic particles, that spend most of their time in the upper flow layers where they can gain momentum from the flow.

Particle dynamics due the interaction between a breaking-induced and a nearbed vortex

M. Brocchini[1], M. Postacchini[1], F. Marini[1], G. Zitti[1], Z. Xie[2] and M. Falchi[3]
[1] DICEA, Università Politecnica delle Marche (Italy)
[2] School of Engineering, Cardiff University (UK)
[3] National Research Council, CNR-INM (Italy)

During wave breaking, vorticity is generated at the air-water interface, and surface vortices typically move downward, as an effect of either spilling or plunging breakers in a 2D or 3D fashion. Further, sharp discontinuities in the seabed promote flow separation and generation of nearbed vortices, as in correspondence of submerged sandbars or man-made defense structures. Such vortices can suspend and transport granular particles with different size and density, like sediments or micro plastics. The interaction between surface (breaking-induced) vortices and nearbed structures is an important link between the upper and lower boundaries of the wave body and leads to complex patterns of tracers' transport.

To inspect the above dynamics, laboratory tests have been performed at the Università Politecnica delle Marche (Italy). A 50 m-long wave flume hosts a 2D physical model made of contiguous sloping platforms (Brocchini et al., 2022). The trajectories of slightly negative buoyant particles (d_p=1.1 g/cm^3; St≈10^{-4}) are reconstructed using the PTV technique on populations of images acquired at 435 fps. The reconstructed trajectories highlighted the interaction between surface and nearbed vortices (Fig. 1a). After the analysis of the Lagrangian normalized velocity autocorrelation, the Taylor length scale has been computed to be around 0.084 m.

Numerical simulations are also run, using the in-house code Xdolphin3D (Xie et al., 2020) to replicate and extend the range of parameters of the experimental tests. 2D RANS simulations have been performed to check the interaction between vortices shoreward of the discontinuity (Fig. 1b), while 3D LES are being undertaken to inspect 3D complex vortical structures. From the reconstructed experimental/numerical velocity fields, the trajectory patterns of Fig.1c have been selected as the most relevant for the illustration of fundamental dynamics involved in the phenomenon.

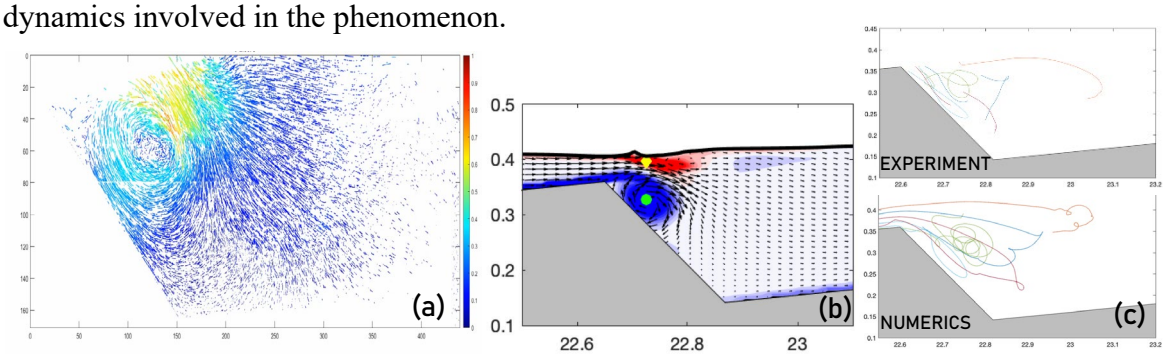

Figure 1: Trajectories of particles from the PTV analysis (a); vorticity field from numerical test (b); reconstructed trajectories from experiment and from numerical simulations (c).

References

M. Brocchini, F. Marini, M. Postacchini, G. Zitti, M. Falchi & Z. Xie (2021). Interaction between breaking-induced vortices and nearbed structures. Part 1: experimental and theoretical investigation. *Journal of Fluid Mechanics*, under peer review.

Z. Xie, T. Stoesser, S. Yan, Q. Ma & P. Lin (2020). A Cartesian cut-cell based multiphase flow model for large-eddy simulation of three-dimensional wave-structure interaction. *Computers & Fluids* **213**, 104747.

Shallow gravity-driven sediment-laden flows

Darish Jeswin Dhas[1] and Anubhab Roy *[1]

[1]Department of Applied Mechanics, Indian Institute of Technology Madras, Chennai 600036, India

Shallow free-surface flows laden with negatively buoyant particles are ubiquitous in various natural settings such as oceans, rivers and estuaries. When devoid of any underlying microstructure, shallow gravity-driven flows are susceptible to a long-wave surface mode instability (Yih 1963) and a shear mode instability (Kelley 1989). The presence of sediment particles alters the local density and viscosity, and imparts additional normal stresses to the carrier phase.

We study the role of sediment particles on the dynamics of a shallow gravity-driven free-surface flow. In such systems, two distinct physics dictate the dynamics of the particle phase - shear-induced migration and buoyancy forces. Shear-induced migration would lead to particle motion towards regions of lower shear-rate, namely the free surface, whereas buoyancy forces would lead to particle settling towards the substrate. The competition between the two physics would thus lead to a non-uniform density and viscosity stratification in the system. We use the constitutive models based on the suspension balance model (Nott & Brady 1994, Morris & Boulay 1999, Frank et al. 2003) to incorporate the physics of shear-induced particle stresses and obtain the base-state velocity and concentration profiles. Subsequently, we perform a linear stability analysis to study the modification to the shear and surface modes of instability due to the presence of sediment particles. Our study reveals that the presence of the particulate phase can enhance the instabilities in gravity-driven free surface flows.

*anubhab@iitm.ac.in

Experiments on a large intruder rising in bedload sediment transport

Benjamin Dedieu*[1], Hugo Rousseau[2, 3], Philippe Frey[1], and Julien Chauchat[4]

[1] *Univ. Grenoble Alpes, INRAE, UR ETNA*
[2] *University of Zurich, Department of Geography*
[3] *EPFL Lausanne, Snow and Avalanche Simulation Laboratory SLAB*
[4] *Univ. Grenoble Alpes, LEGI*

Vertical size segregation or sorting of particles in bedload transport, strongly impacts the sediment rate and the river bed morphology. To better account for this process in sediment transport models, it is essential to understand the mechanisms acting at the grain scale (Frey and Church, 2009). Following the work of Rousseau (2021), focus is made on the behaviour of a single large particle segregating upwards in a monodisperse mixture of smaller beads during bedload transport. Experiments are carried out in a narrow flume and the bead dynamics is recovered through image analysis (Figure 1). The time for the large particle to reach the bed surface increases with the size ratio (large to small bead diameter). This result supports previous research which, using simpler granular configurations, evidenced a similar tendency in terms of segregation force (Guillard et al., 2016; Jing et al., 2020) or segregation velocity (Golick and Daniels, 2009). On the contrary, the spatial trajectory of the intruder does not appear to change with the size ratio. Indeed a linear trajectory is observed with a repeatable slope independent of the size ratio. These observations offer interesting insights to understand the mechanisms governing size segregation and could provide new closures to upscale the phenomenon at the continum scale.

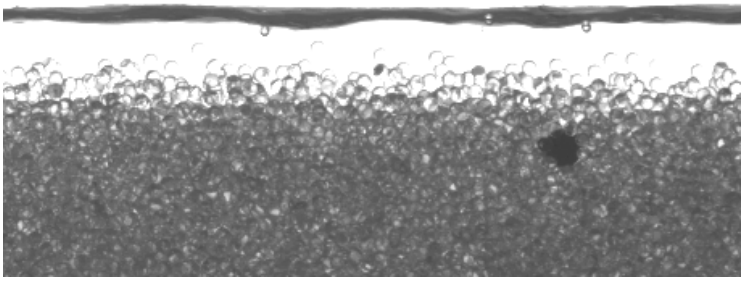

Figure 1: A 5.1 mm intruder in a 2 mm bed (size ratio = 2.55), flow from right to left, dimensionless bed shear stress (Shields number) = 0.25.

Frey, P. and Church, M. (2009). "How River Beds Move". *Science*, 325(5947), pp. 1509–1510.

Golick, L. A. and Daniels, K. E. (2009). "Mixing and Segregation Rates in Sheared Granular Materials". *Physical Review E*, 80(4), p. 042301.

Guillard, F., Forterre, Y., and Pouliquen, O. (2016). "Scaling Laws for Segregation Forces in Dense Sheared Granular Flows". *Journal of Fluid Mechanics*, 807.

Jing, L., Ottino, J. M., Lueptow, R. M., and Umbanhowar, P. B. (2020). "Rising and Sinking Intruders in Dense Granular Flows". *Physical Review Research*, 2(2), p. 022069.

Rousseau, H. (2021). "From Particle Scale to Continuum Modeling of Size Segregation in Bedload Transport : A Theoretical and Experimental Study." PhD thesis. Université Grenoble Alpes.

Rousseau, H., Frey, P., and Chauchat, J. (2022). "Experiments on a single large particle segregating in bedload transport". *Physical Review Fluids*. in review.

*Corresponding author: benjamin.dedieu@inrae.fr

A NUMERICAL STUDY OF SWASH AND BEACH GROUNDWATER INTERACTIONS

Marie-Pierre Delisle, University of California, Los Angeles, USA, mpdelisle@g.ucla.edu
Yeulwoo Kim, Pukyong National University, Busan, South Korea, yarkim@pknu.ac.kr
Timu Gallien, University of California, Los Angeles, USA, tgallien@seas.ucla.edu

Coastal flooding is a growing socioeconomic and humanitarian hazard. Sea level rise will raise beach groundwater levels, potentially inundating low-lying areas from groundwater exposure while simultaneously propagating swash impacts onto higher beach and backshore elevations. Conventional cross-shore Boussinesq or nonlinear shallow water based numerical models characterize only surface flows and neglect key swash zone processes associated with the sediment bed such as infiltration/exfiltration. Intrinsically, swash zone flows are multi-phase, shallow, and transient imposing numerous modeling and observational challenges. In this study, the free-surface resolving Reynolds-averaged Eulerian two-phase sediment transport model, SedWaveFoam, is integrated with the surface wave generator, olaFlow, in the OpenFOAM framework. The new model, SedOlaFlow, is applied to a dam-break generated swash event on a flat, sloping beach with a fixed, porous sediment bed. SedOlaFlow is validated with measured laboratory flume observations (Kikkert et al., 2013). Preliminary results show that the modeled free surface elevation agrees well with measured data (Figure 1). Model validation includes shoreline position, velocity, and turbulent kinetic energy. Modeling suggests that antecedent groundwater levels substantially impact uprush excursion extent and duration.

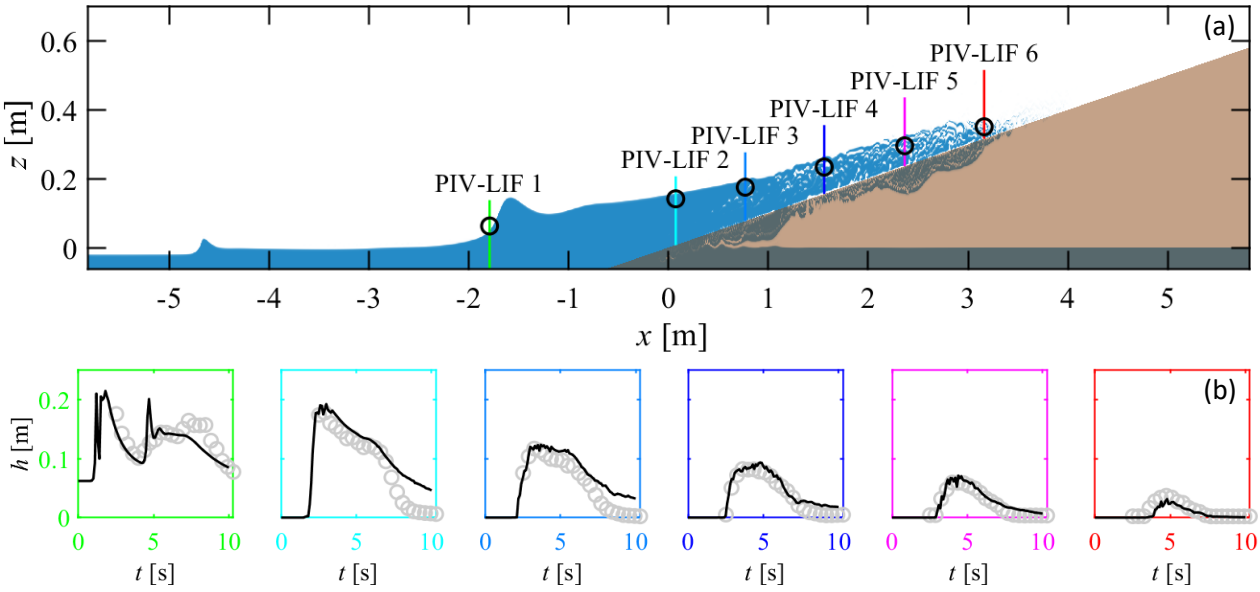

Figure 1. (a) Snapshot of numerical flume during uprush, ~2.7 s after bore arrival at toe (circles, measured data). Air, surface water, groundwater, and sediment phases are white, blue, dark blue/grey, and brown, respectively. The colored vertical lines indicate the cross-shore deployment location of PIV-LIF sensors for water depth and velocity profiles at x = -1.79 m (green), 0.07 m (light blue), 0.77 m (blue), 1.56 m (purple), 2.37 m (pink), and 3.16 m (red). (b) Time series of measured (grey circles) and modeled (black, solid curve) water depth (h) at the PIV-LIF sensor locations marked in (a) using the corresponding color.

Title: Suspended sediment concentration and sediment transport measurements with a two components ultrasonic profiler

Authors: Helder Guta, Marie Burckbuchler, Stéphane Fischer

Measuring velocity profiles in turbulent flows has always been of great theoretical and practical interest. It allows the statistical characterisation of turbulence and better understanding of processes such as sediment motion, closely related to the flow turbulence. A full agreement on how turbulent flows are affected by presence of particles is yet to be reached. An example is the modification of the well-known law of the wall, which has been the subject of analysis by several authors [1]. Several studies report a reduction of the von Karman parameter in mobile-bed flows, however, the full description of these modifications according to the sediment-laden flow regime is not available. Another question lies in understanding the behaviour of turbulent bursting events. They are reported [2] to be very important on the suspension dynamics.

Over the past two decades, the development of increasingly sophisticated measuring systems has enabled flow parameters to be obtained from acoustic technology. For example ADCPs (Acoustic Doppler Current Profilers) or UVPs (Ultrasonic Velocity Profilers) are based on multiple diverging monostatic configuration. These profilers are capable of reasonable to high temporal and spatial resolutions and have been increasingly used in the fields of research and environmental engineering. Yet, none of these devices allow to resolve sufficiently fine flow scales, preventing a proper characterization of turbulence statistics and turbulent processes. To overcome these limitations, ADVPs (Acoustic Doppler Velocity Profilers) were developed [3] to provide quasi-instantaneous co-located two (2C) to three (3C) components velocity profiles along the transmitter beam axis, using a multi-bistatic configuration. These devices were shown to resolve up to the Taylor microscale.

In 2019, Ubertone developed a commercial version of the ADVP, the UB-Lab 2C, as part of the ANR ASTRID selected in 2017 project MESURE (Métrologie mES hydroacoUstiques opéRationnElles).

In the present paper, datasets of time-resolved two components velocity profile measurements under different flow conditions will be presented.

In particular, the comparison campaign between the UB-Lab 2C and the well-established ACVP developed by the LEGI (France) was carried out under steady uniform turbulent rough clear water and sheet-flow. Taking into account flow condition differences in the tilting flume with sediment pit, the results of this measurement campaign demonstrates the good performance of the commercial ADVP compared to the ACVP, in clear water and sheet-flow.

This paper will remind the already shown capabilities of this measurement technique ADVP, such as its good performance for sediment flux profiling. And we will present new results and new potential and developments around these instruments, such as a commercial 3C-ADVP.

[1] Revil-Baudard T, Chauchat J, Hurther D. and Barraud P A, Investigation of sheetflow processes based on novel acoustic high-resolution velocity and concentration measurements. J. Fluid Mech. 767, 1–30, 2015.

[2] Nezu I. and Nakagawa H, Turbulence in Open-channel Flows. (Rotterdam, Balkema), 1993.

[3] Hurther D, Thorne P D, Bricault M, Lemmin U and Barnoud J M, “A multifrequency acoustic concentration and velocity profiler (ACVP) for boundary layer measurements of fine-scale flow and sediment transport processes”, Coastal Engineering. 58, 594–605, 2011.

Grain-size segregation in bed-load transport on steep slopes.

Philippe Frey, Rémi Chassagne, Hugo Rousseau, and Julien Chauchat

We report on an ongoing research effort on bedload transport multi-scale size segregation modelling within the framework of the ANR project SegSed (size **Seg**regation in **Sed**iment transport). Using a combination of laboratory flume experiments and a coupled fluid-discrete element model, it was possible to carry out 'real' and 'numerical' experiments on a variety of bedload bidisperse and intruder configurations, probing the depth structure and the segregation dynamics. Comparing to 'real' laboratory experiments, discrete models allow access to the internal morphodynamics and to variables difficult to measure in the laboratory. These variables permit deriving or calibrating constitutive relationships and size segregation equations. Upscaling from discrete element methods to continuum models, these relationships could be implemented in Eulerian-Eulerian two-phase flow models. Ultimately as a perspective, such studies should be useful to improve Exner-shallow water-type models, used at larger scales, especially when grain sorting is considered.

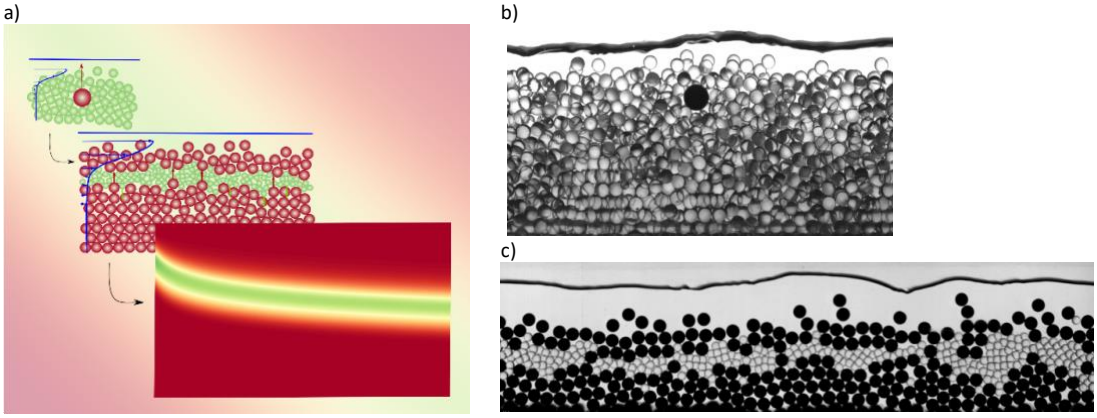

Figure. a) From discrete methods to a continuum model (Rousseau et al. 2021) b) An intruder moving upwards in a 5-mm bedload flow, size ratio of 1.8 (Rousseau et al. in revision) c) Segregation of bidisperse bedload mixtures, 4 and 6mm bead diameters (Frey et al.2020). b) and c) experiments in a narrow flume.

Chassagne R, Frey P, Maurin R, Chauchat J. 2020. Mobility of bidisperse mixtures during bedload transport. *Physical Review Fluids* **5**(11): 114307.

Chassagne R, Maurin R, Chauchat J, Gray JMNT, Frey P. 2020. Discrete and continuum modelling of grain size segregation during bedload transport. *Journal of Fluid Mechanics* **895**: A30.

Frey P, Lafaye de Micheaux H, Bel C, Maurin R, Rorsman K, Martin T, Ducottet C. 2020. Experiments on grain size segregation in bedload transport on a steep slope. *Advances in Water Resources* **136**: 103478.

Maurin R, Chauchat J, Chareyre B, Frey P. 2015. A minimal coupled fluid-discrete element model for bedload transport. *Physics of Fluids* **27**(11): 113302.

Rousseau H, Chassagne R, Chauchat J, Maurin R, Frey P. 2021. Bridging the gap between particle-scale forces and continuum modelling of size segregation: Application to bedload transport. *Journal of Fluid Mechanics* **916**: A26.

Coarse and fine sand transport processes in the ripple vortex regime under asymmetric nearshore waves.

Noémie Fritsch [1], Guillaume Fromant [2], David Hurther [3], Ivan Cáceres [4].

1. Laboratoire de Géosciences Océan, Université de Bretagne Occidentale, Brest, France.
2. Laboratoire d'Informatique Signal et Image de la Côte d'Opale, Calais, France.
3. Laboratoire des Ecoulements Géophysiques et Industriels, Grenoble, France.
4. Universitat Politècnica de Catalunya, Barcelone, Espagne.

Precise sand transport modelling and process-based parametrization are needed for improved long-term predictions of coastal morphology evolution in the context of increasing anthropic activity. In particular, ripple vortex regime modelling still presents shortcomings, despite the fact that sand ripples are common bedforms found all across the oceanic nearshore region. In particular, the agreement between experimental data and model predictions of sand ripple dimensions is still considered as poor from a quantitative point of view. In the present study, an ACVP (Acoustic Concentration and Velocity Profiler) and other flow measurement tools were deployed in the CIEM wave flume of Barcelona (HYDRALAB-RIPCOM) to collect high-resolution concentration and velocity profile data above coarse sand ripples generated under regular asymmetric nearshore waves. Intrawave, intraripple and net contributions of sand transport rates are discussed for both the bedload and suspended load contributions. In particular, the detailed ripple vortex dynamics on either side of the ripple crest is analyzed in relation to acceleration skewness. The obtained results are compared to the recent study of Wang and Yuan (2020) conducted in acceleration skewed oscillatory flows for coarse sand ripples. Moreover, the differences are highlighted in terms of ripple vortex dynamics, associated sand entrainment, net bedload and suspended load sand fluxes compared to the well documented ripple vortex regime under velocity skewed oscillatory flows (van der Werf et al. 2007, 2008, Salimi-Tarazouj et al. 2021) and skewed shoaling waves (Hurther and Thorne 2011). Finally, differences seen between coarse and fine sand experiments are discussed in terms of ripple vortex processes inside the Wave boundary Layer. This work offers new perspectives for process-based parametrization of sand transport models in the ripple vortex regime and highlights the need to collect high-resolution in situ data, since field experiments under irregular waves are lacking.

WAVE BOUNDARY LAYER AND SHEETFLOW PROPERTIES UNDER LARGE-SCALE BREAKING WAVES

G. Fromant, Laboratoire des Ecoulements Géophysiques et Industriels / Laboratoire d'Informatique, Signal et Image de la Côte d'Opale, guillaume.fromant@univ-littoral.fr
D. Hurther, Laboratoire des Ecoulements Géophysiques et Industriels, david.hurther@legi.cnrs.fr
J. van der Zanden, J.S. Ribberink, University of Twente, j.vanderzanden@utwente.nl, j.s.ribberink@utwente.nl
D. van der A, T. O'Donoghue, University of Aberdeen, d.a.vandera@abdn.ac.uk, t.odonoghue@abdn.ac.uk
I. Cáceres, Laboratori d'Enginyeria Maritima, Universitat Politècnica de Catalunya, Spain

In the present study, we examine the wave bottom boundary layer (WBL) hydrodynamics and sheet-flow properties measured with an Acoustic Concentration & Velocity Profiler (ACVP) (Hurther et al. 2011) at 5 cross-shore locations across the wave breaking region of regular large-scale plunging-type breaking waves. The nearly full-scale wave flume experiment allowed a wave-driven flow condition in the same turbulent rough flow regime as the one found on natural beaches. The results show that in the shoaling zone the near bed orbital velocity field is similar to previous non-breaking wave observations in terms of wave shape characteristics, intra-wave and maximum WBL thickness and velocity phase lead. The WBL hydrodynamics exhibit locally bed friction dominated characteristics in very good agreement with those obtained in purely skewed and purely asymmetric oscillatory flows. The observed sheet flow properties in terms of intra-wave and maximal erosion depth, sheet flow layer thickness, and intra-wave concentration dynamics reveal the existence of a lower pick-up layer and an upper sheet-flow layer with properties similar to those documented for skewed oscillatory sheet flows. Using the full measurement performance of the ACVP technology, the direct measurements of the net bedload flux profiles and transport rates were decomposed into current-, wave-, and turbulence-driven components. In the shoaling region, the sand transport is found to be fully dominated by the onshore skewed wave driven component with negligible phase lagging effects. In the outer surf zone, the total net flux exhibits a 3-layer vertical structure typical of skewed oscillatory sheet-flows subject to phase lag effects (O'Donoghue and Wright (2004)). However, the decomposed profiles show that this structure originates from a misbalance between an offshore-directed undertow driven flux and an onshore-directed wave driven flux, with negligible of phase lagging effects. Finally, at the plunge-point position, the turbulence driven onshore component becomes significant enough to balance the offshore directed wave and current contributions.

Inertial effects in shear-driven immersed granular flows

B. Fry*, L. Lacaze*, T. Bonometti*, F. Charru*

We here consider the steady transport of a bed of grains by a laminar Couette flow. The main question addressed here concerns the relevance of mesoscale models, for which the granular phase is modelled as a continuum phase, for this specific flow. Numerical simulations are thus performed at the so-called microscale at which individual grain dynamics is resolved, using an Immersed Boundary Method (IBM) coupled to a Discrete Element Method (DEM) granular solver. Up-scaling is then performed to describe the flow at the mesoscale. Simulations cover a grain-to-fluid density ratio of 2.5, a range of particle Reynolds numbers $Re_p \in [0.1,\ 10]$ and Shields numbers $\theta \in [0.1,\ 0.7]$. We found that the apparent rheology of the fluid phase depends on $\sqrt{Re_p}\theta$. This dependence is attributed to some inertial effects at the grain scale. On the other hand, the rheology of the granular phase is found independent of Re_p and θ and well described by a viscoplastic model of $\mu - I$ type. Our results also show that the apparent viscosity of the mixture phase is well described by both the classical Krieger and Dougherty (1959)'s empirical law and the more recent phenomenological model of Boyer et al. (2011). A model for the effective viscosity of the mixture, taking into account the $\sqrt{Re_p}\theta$ dependency, is proposed based on previous experimental results as the sum of the effective viscosities of these two equivalent phases. This model is shown to predict reasonably well the mixture effective viscosity obtained from the microscale simulations.

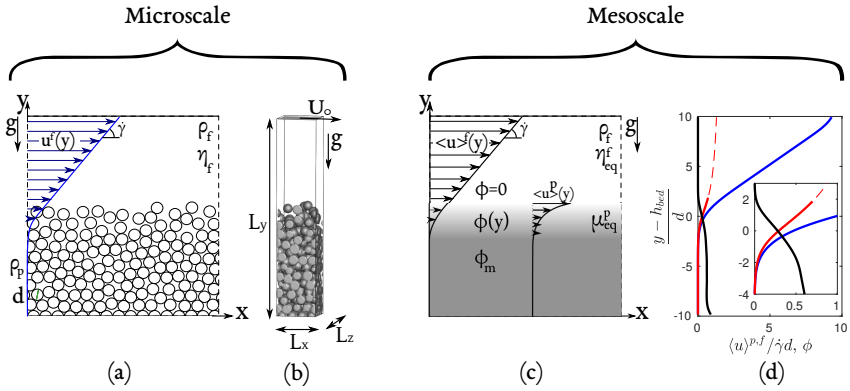

Figure 1: (a): Scheme of the problem at the microscale. (b): Simulation domain. (c): Problem at the mesoscale. (d): Vertical profile of the streamwise velocity in the fluid phase (blue, $\langle u \rangle^f$), the granular phase (red, $\langle u \rangle^p$) and solid volume fraction (black, ϕ) for $Re_p = 1$ and $\theta = 0.67$. The velocity profile of the granular phase is represented with a solid line for $\phi \geq 0.025$ and with a dashed line otherwise. The characteristic length of the weighting function for the upscaling is $h_g = d$. h_{bed} is the mean height of the granular bed defined as the barycentre of the local granular flow rate as suggested by Duran et al. (2012).

*Institut de Mécanique des Fluides de Toulouse, IMFT, Université de Toulouse, CNRS - Toulouse, FRANCE

Experimental lock-release turbidity currents: slope, volume fraction and settling velocity.

C. Gadal[1], M. Mercier[1], and L. Lacaze[1]

[1]Institut de Mécanique des Fluides de Toulouse (IMFT), Université de Toulouse, CNRS, INPT, UPS, Toulouse, France

Turbidity currents are buoyancy-driven-flows whose driving agent resides in the presence of suspended particles.Their motion can originate from the sudden release of a finite volume of heavy particles in air or water or by a continuous discharge of negative buoyancy source. They are present in both industrial (food, water management, pharmaceutical) and natural (snow avalanches, sandstorms, pyroclastic flows) situations. At the scale of the current, fluid displacement in buoyancy-driven-flows is mostly governed by a single parameter, the Froude number. However, the presence of particles in turbidity currents, as opposed to temperature- or salinity-driven gravity currents, induces related processes such as sedimentation, flow-particle interactions and particle-particle interactions. Depending on the particle and flow properties, these processes can drastically alter the current morphodynamics.

We present here lock-release experiments of turbidity currents for varying slopes (1° – 7°), volume fractions (0.5 % – 15%) and silicate particle diameter (sand and glass beads, 60 μm – 200 μm). On the upstream side of the tank, particles are suspended by stirring behind a locked door. At the beginning of the experiment, the agitation is stopped and the door opened, releasing the suspension which then flows downwards. By following its dynamics using a camera at 120 Hz, we extract time series of the current shape and position. In this presentation, we will discuss results based on the evolution of the front dynamics, including its velocity and typical height, as well as of the flow cessation induced by particle deposition, depending on the initial control parameters: slope, volume fraction and particle diameter.

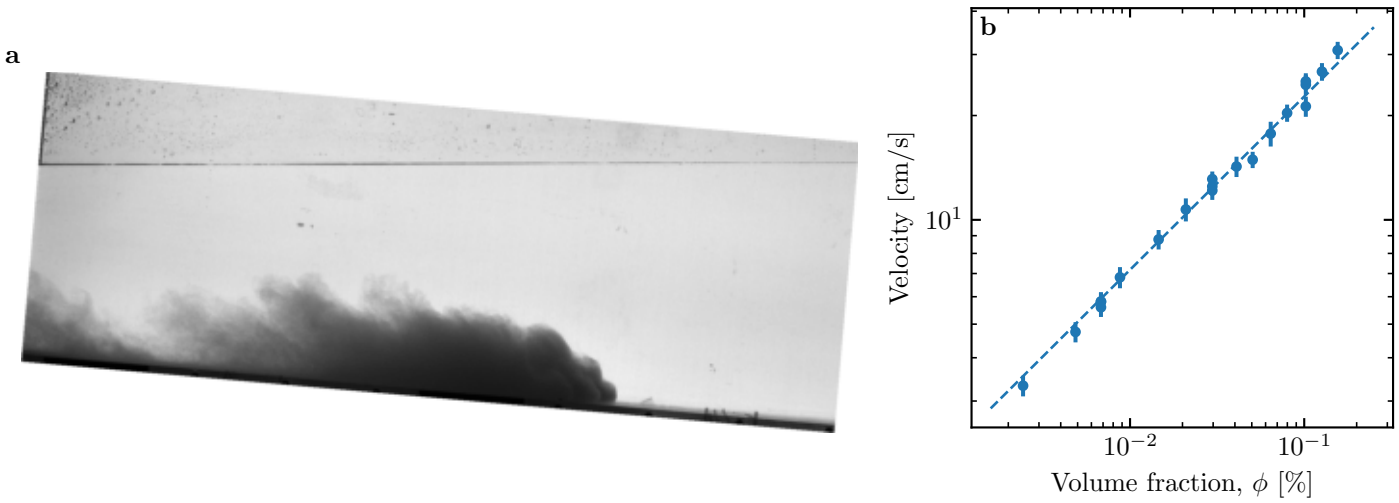

Figure 1: Turbidity currents with 80 μm sand on a 5° slope. **a**: experimental image. **b**: scaling of the initial velocity.

Title : Towards turbulence-resolving two-fluid simulation of scour process

Authors : Alban Gilletta de Saint Joseph (FEM/LEGI), Julien Chauchat (LEGI), Cyrille Bonamy (LEGI) and Marie Robert (FEM)

In the context of energetic transition in France, renewable energy is highly promoted aiming at reaching carbon neutrality in 2050. Offshore Wind Farms (OWF) are amongst the most efficient alternatives to complement the national energetic mix plan and the first OWF is commissioned for the end of the year 2022, far behind many other European countries. Implementation of OWF is very challenging due to technical aspects notably the stability of foundations in the sediment bed (Soares-Ramos et al., 2020) where under the action of waves and currents, the process of scour may lead to the failure of the structure.

The flow around a wall-mounted circular cylinder has been extensively studied in the literature in various contexts including river and coastal engineering (bridge, pier or offshore wind turbine pile). The presence of the cylinder and of the bottom is responsible for the generation of a variety of vortices such as the horseshoe-vortex (HSV) upstream and shedded vortices downstream. The emergence of these vortices are controlled by two dimensionless numbers: the Reynolds number (Re_D) comparing inertia force over viscous force and the Keulegan-Carpenter number (KC) comparing drag forces over inertia force. Many numerical studies have been been carried out to simulate these phenomena using different turbulence modeling approaches such as Reynolds-Averaged Navier-Stokes equations (RANS), Large Eddy Simulation (LES) and hybrids RANS-LES. For a steady current around a cylinder, the three turbulence modeling approaches have been compared with experimental data (*e.g.* Roulund et al., 2005; Kirkil and Constantinescu, 2015). Unsteady RANS simulations allows to reproduce the mean flow field reasonably well at an affordable computational cost, still it can not reproduce accurately the vortex dynamics around the structure and in particular the dynamics of the HSV which exhibits a bimodal oscillation (Roulund et al., 2005; Nagel, 2020) and leads to an underpredicted scour depth in front of the pile. This behavior is well captured by hybrid RANS-LES and LES turbulence models (Kirkil and Constantinescu, 2015). In these later approaches, one of the key issue is to impose a realistic turbulence at the inlet (Kirkil and Constantinescu, 2015). In the present contribution, we evaluate the Divergence Free Synthetic Eddy Method (DFSEM - Poletto et al., 2013) available in openFOAM to force the turbulence at the inlet. Hydrodynamic simulations have been performed at very coarse, coarse and medium resolutions (dx+~250-100 ; dy+~250-100 ; dz+~4-2) using the solver pimpleFOAM with the k-omegaSST, k-omegaSSTIDDES, Smagorinsky and dynamic Lagrangian Smagorinsky models. Our results shows that the hybrid k-omegaSSTIDDES and the dynamic Lagrangian Smagorinsky models are able to reproduce the bimodal oscillation of the HSV, whereas RANS can not. Concerning the vortex-shedding, all approaches reproduce reasonably well the vortices dynamics but with a better accuracy when using LES of course. Hybrid RANS-LES with coarse resolution seems to be a good compromise to capture the main flow features at an affordable computational cost. LES evaluated in this first step has been used to simulate scour using the two-fluid model (e.g. sedFOAM) in the continuity of Tim Nagel's PhD work (Nagel 2018, Nagel et al. 2020). Preliminary results will be presented at the conference.

E. P. P. Soares-Ramos, L. de Oliveira-Assis, R. Sarrias-Mena, L. M. Fernandez-Ramirez. Current status and future trends of offshore wind power in Europe. *Energy*, 202 (2020) 117787.

R. Poletto, T. Craft, and A. Revell. A New Divergence Free Synthetic Eddy Method for the Reproduction of Inlet Flow Conditions for LES. *Flow, Turbulence and Combustion*, 91(3):519–539, 2013.

A. Roulund, B. M. Sumer, J. Fresoe and J. Michelsen. Numerical and experimental investigation of flow and scour around a circular pile. *Journal of Fluid Mechanics*, (2005), vol. 534, pp. 351-401.

G. Kirkil and G. Constantinescu. Effects of cylinder Reynolds number on the turbulent horseshoe vortex system and near wake of a surface-mounted circular cylinder. *Physics of Fluids*, 27, 075102 (2015).

T. Nagel, J. Chauchat, C. Bonamy, X. Liu, Z. Cheng, T.-J. Hsu. Three-dimensional scour simulations with a two-phase flow model. *Advances in Water Resources*, 138 (2020) 103544.

Nagel, T. (2018), Numerical study of multi-scale flow-sediment structure interactions using a multi-phase approach, Ph.D. thesis, University of Grenoble Alpes.

Near-bed sediment transport during bar migration in large-scale experiments

Authors: Florian Grossmann (UPC Barcelona), David Hurther (LEGI, CNRS, Grenoble) and Jose Alsina (UPC Barcelona)

The morphological evolution of natural beaches is based on sediment transport processes. To forecast the evolution, the processes must be mathematically modelled and sediment transport calculated. In this context, various transport formulations exist (e.g. van der A et al., 2013) but most of the data, which they were developed upon, was measured under erosive wave conditions. Such conditions are linked to net offshore sediment transport and beach erosion. For long term morphological development, accretive conditions, characterized by net onshore transport, onshore bar migration and beach recovery, are equally important but related data is scarce. Therefore, it is not surprising that mathematical modeling of morphological evolution under accretive waves is deemed less accurate.

During the HYDRALAB+ transnational access project "Influence of storm sequencing and beach recovery on sediment transport and beach resilience" (RESIST), large-scale (1:1) experiments were conducted in the CIEM wave flume at UPC Barcelona. The experiments featured fully evolving beach profiles (D_{50}=0.25mm, starting from an initial slope of 1:15) under precisely-repeatable bichromatic erosive and accretive wave groups. Measurements of suspended and bedload sediment flux profiles (co-located concentration and velocity) were conducted with state-of-the-art instrumentation (Hurther et al., 2011) at particularly high resolution near the bed.

The data shows that bedload is fundamental for net onshore transport. Suspended transport mainly contributes to net offshore transport. But, when offshore-directed undertow is low and onshore-directed streaming high, it also contributes net onshore transport. Whereas suspended load is related to time-averaged currents, bedload is related to short wave motion. As transport from infragravity waves only takes a minor role in the present experiments, total net transport is mainly determined by bedload, short wave-related transports and suspended, current-related transports. Their balance changes with wave condition (erosive or accretive) and cross-shore location (offshore or onshore of breaker bar).

Transport formulations consider the mentioned transport components at varying degrees of sophistication but comparisons with accretive sediment transport data are scarce. In our contribution we present such comparisons, analyzing why certain formulations perform better than others under the accretive and erosive wave conditions. Furthermore, we present the correlation of concentration and sediment transport measurements with a variety of hydrodynamic quantities, which might serve as the basis for transport formulations. This provides useful information for further development of two-phase flow models to forecast long-term morphological evolution under consideration of accretive time periods.

References

Hurther, D. et al., 2011. A multi-frequency Acoustic Concentration and Velocity Profiler (ACVP) for boundary layer measurements of fine-scale flow and sediment transport processes. Coastal Engineering 58 (7), 594-605. doi: 10.1016/j.coastaleng.2011.01.006

Van der A, D. A. et al., 2013. Practical sand transport formula for non-breaking waves and currents. Coastal Engineering 76, 26-42. doi: 10.1016/j.coastaleng.2013.01.007

Experimental study of turbulent suspension processes in energetic open-channel flows

Hélder Guta[1], David Hurther[1], Julien Chauchat[1]

[1]LEGI, University of Grenoble Alpes, G-INP, CNRS, 38000 Grenoble, France

A process-based analysis of a new experimental dataset is carried out based on co-located 2C velocity, sediment concentration and sediment flux profile measurements obtained with an Acoustic Concentration and Velocity Profiler (ACVP). The experiments were carried out in energetic open-channel flows using the LEGI tilting flume, with light-weight PMMA of two diameters dp=3mm (covering the range suspension numbers, given as the ratio of settling velocity ws and friction velocity u_* 0.8≤ws/Uf≤1.3 and Shields number 0.35≤θ≤0.85,) and dp=1mm (0.4≤w_s/u_* ≤0.6 and 0.4<θ<1). Four sediment-load conditions are studied for a given hydraulic flow varying from clear water, 2 non-capacity to the full transport capacity conditions. Three hydraulic flow conditions are investigated for each particle diameter. All sediment-laden runs have one clear-water run as reference, acquired before each sediment-laden run. This allows the analysis of the particle effects on a wide variety of hydrodynamic quantities. With the larger particle experiments (dp=3mm), it is shown that the bed-load layer has important impact on the turbulent boundary layer. The log-layer is found to prevail only from around the edge of the bed-load layer upwards. Inside this layer, turbulent momentum mixing is highly reduced, compared to the corresponding clear-water flow. It is seen that this change in flow structure should be taken into account in the turbulent mixing length model, affecting both the law of the wall and the Rouse formulation, for modelling velocity and concentration distribution, respectively. As result, a modified analytical solution that includes the bed-load effects for the concentration profile was derived. Concerning the experiments with dp=1mm, less pronounced effects of turbulent mixing length and eddy viscosity were observed. A parametrization of the depth-averaged ratio of sediment and momentum diffusivity β based on the present experimental results was proposed, allowing to extend the van Rijn (1984) model to a wider range of suspension numbers (0.1≤ w_s/u_* ≤1.5). Finally, the differences in the flow structure in the sediment-laden with the two particle diameter is further illustrated through some terms in balance of turbulent kinetic energy and by turbulent coherent structures (specifically ejections and sweeps).

Movement mechanism of boulders composing valley bank and beds by debris flows and development of debris flow front using the APM method

Hiroki Kato, Graduate Student of Science and engineering, Chuo University, Japan.
Email: a17.jnt5@g.chuo-u.ac.jp
Shoji Fukuoka, Professor, Research and Development Initiative, Chuo University, Japan.
Email: sfuku@tamacc.chuo-u.ac.jp

Keyword: *debris flow, one-fluid model of solid-liquid multiphase, APM method, valley bank and bed erosion*

Abstract:

To understand the mechanism of erosion phenomena, it is important to consider how individual particles start to move. Since it is difficult to accurately measure the force relationships between individual particles by field observation and model experiments, numerical experiments are expected to clarify the initiation mechanism. In addition, it is essential to analyze particle motion with a discrete model rather than the conventional continuum model because each particle has a discrete motion in character. Fukuda et al. [1] have developed a model (APM method) in which the fluid is calculated by a continuum model (LES) and the gravel is calculated by a discrete model (DEM). In the APM method, a one-fluid model of solid-liquid multiphase flow is used. In the one-fluid model, the physical properties (density, viscosity) and flow velocity of a cell containing solid and liquid phases are assumed to be volume-averaged and mass-averaged. The volume fraction α of the solid phase is evaluated by the sub-cell method. A mesh of sufficient size to analyze the flow field around the particles is used, and the fluid force acting on the particles is directly calculated by volume integration of the pressure and diffusion terms.

In this study, the APM method was used to investigate the erosion mechanism by particle motions over the valley bed and bank. Our numerical results are similar to the laboratory experimental results of Lyu et al. [2]. From the results of the numerical experiments, it can be seen that both the bed and bank particles receive a large force in the downstream direction from the arrival of the debris flow front, but remain stationary due to the equal resistance due to the surrounding particles. Later, when the surrounding field changed, the particles could not obtain sufficient resistance and started to move. In addition, the particles on the valley bank started to shift according to the movement of just downstream particles. In the case of the particles on the valley bed, the particles themselves moved vertically upward and were positioned relatively higher than the surrounding particles, so they were not able to provide much resistance. Fig.2 shows the velocity contour plot of the central section of the channel. The flow velocity is low in the front and fast in the body. The particles that started to move were transported to the front by the fast body flow, and the front grows larger.

Reference:

[1] Fukuda T. and Fukuoka S., *Advances in Water Resources, Vol.129, pp.297-310*, 2019.
[2] Liqun Lyu., Zhaoyin Wang., Peng Cui. and Mengzhen Xu., *Geomorphology*, *Vol.285, pp.137-151,* 2017.

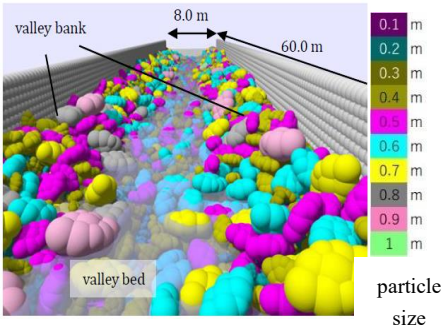

Fig. 1 initial state of numerical

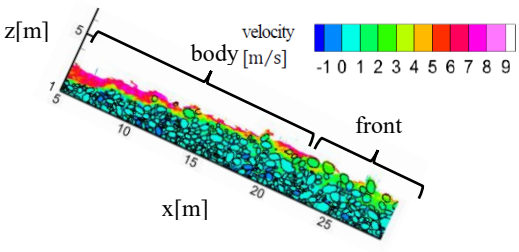

Fig. 2 velocity contour

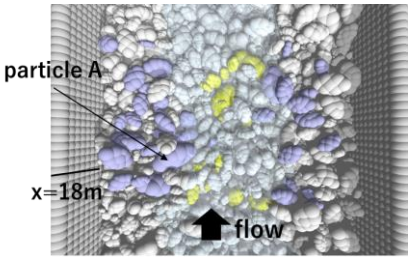

Fig. 3 particle A and its surrounding

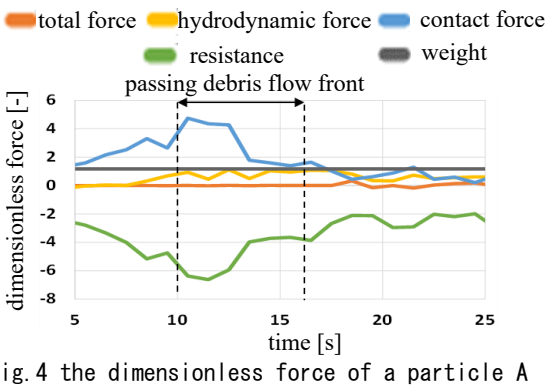

Fig. 4 the dimensionless force of a particle A

Progressive failure of submarine slopes

G. H. Keetels & D. Weij, Delft University of Technology,
THESIS June 2022.

A hardly recognized phenomenon is that underwater sand slopes can stay, temporarily, steeper than the internal friction angle. Under some conditions, this can result in a progressive failure of densely-packed sand slopes. To model this process it is important to incorporate both the pore pressure that develops in the sand body and the turbidity current along the slope. In this contribution a model will be presented that captures both of these soil mechanical and fluid mechanical features in a single computational framework. The model results will be compared with experimental data.

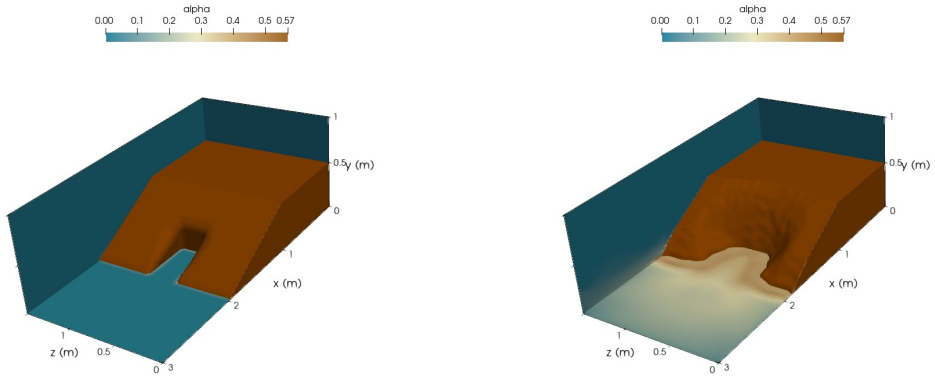

Figure 1: Failure of a densely-pack sand slope with an initial disturbance (a) and progressive failure after t=15 s (b). Colors indicate the solids phase fraction alpha.

reference

D. Weij, On the modelling of the unstable breaching process, PhD-Thesis Delft University of Technology (2020).

Abstract for THESIS conference 2022

Modeling of the interactions between hydrokinetic turbines and bedforms using the two-phase Euler-Euler approach

F. Khaled[1,3], S. Guillou[1], Y. Mear[1,2], F. Hadri[3]

fatima.khaled@unicaen.fr ; sylvain.guillou@unicaen.fr ; yann.mear@lecnam.net *; ferhat.hadri@uvsq.fr*

[1] Normandie Université, UNICAEN LUSAC, EA 4253, 60 rue Max Pol Fouchet, CS 20082, 50130 Cherbourg

[2] INTECHMER, Bd de Collignon, 50110, Tourlaville

[3] LISV, Université de Versailles, 78140 Vélizy

Accelerating hydrokinetic renewable energy development towards endurance requires investigating interactions between the hydrokinetic turbine and its surrounding physical environment. Interactions between hydrokinetic turbines (HT) and mobile sediment bed are considered as a critical area of assessment, however limited research studies have been published to address this issue. Hill et al. (2015) have shown experimentally that the presence of either single or multiple turbines and the rotation of the blades affect the bed morphology. Musa et al. (2019) have investigated experimentally the local effect of streamwise aligned turbines on the bedload, they found as a result that the geomorphic effects are stronger with increasing shear stress due to the presence of the rotors, inducing an alternating scour-deposition phenomenon. Chen et al. (2017) have investigated the influence of rotor blade tip clearance (distance between blades and seabed) on the scour rate of pile-supported horizontal axis tidal current turbine. The results suggest that the decrease in tip clearance increases the scour depth, hence more sediment transport. Recently, Khaled et al. (2021) have studied the impact of hydrokinetic turbine on erodible sand banks, they showed numerically a significant interaction between the confinement of the turbine and its impact on the near bottom.

In the present issue, we study the impact of two interacted turbines on the near bedform morphology. A modelling framework is derived to predict the significant transport induced by the turbines, such as the Euler-Euler (EE) multiphase model for sediment transport and the Blade Element Momentum Theory (BEMT) to model the forces generated by the turbines, using the open source platform OpenFOAM and the library SedFoam (Chauchat et al. 2017). A phase of validation is presented for BEMT using the experiments of Mycek et al. (2014) (fig. 1) then for the combined model (EE and BEMT) using those of Hill et al. (2015). The present study consists in considering one sediment class, sand of diameter of 0.25 mm, and two horizontal axis turbines with an axial flow direction corresponding to the riverine case. The approach is configured with four different axial inter-turbines distances: configurations A_1, A_2, A_3 and A_4 .The wake distribution behind the second turbine is altered by the wake of the upstream turbine in all configurations (fig. 2). This interaction promotes the erosion under the turbines and the deposition along the axis of the turbines in the wake due to relation between the dynamics of ripples generation and the wake effects of turbines (fig. 3).

Keywords: *Numerical simulation, Euler-Euler multiphasic, Hydrokinetic turbines, sediment transport, BEMT, OpenFOAM.*

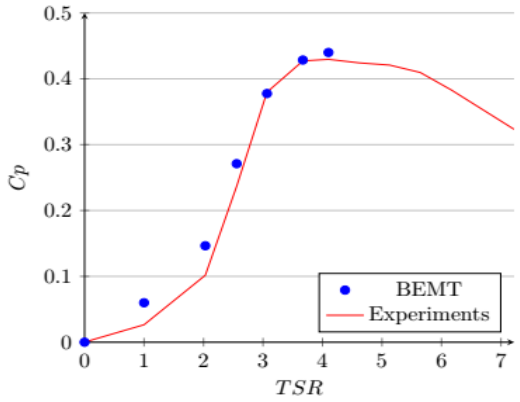

Figure 1: Variation of the power coefficients generated by the turbine in function of the velocity, comparison between the present numerical results (BEMT) and the measurements of Mycek et al. (2014).

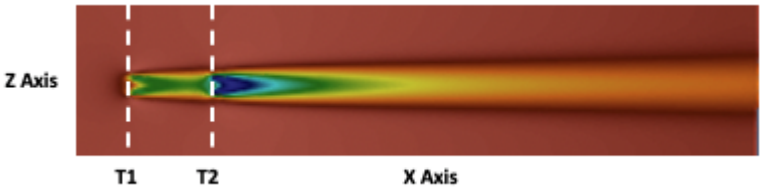

Figure 2: Axial wake distribution showing the interaction between two turbines 4 turbine diameters apart.

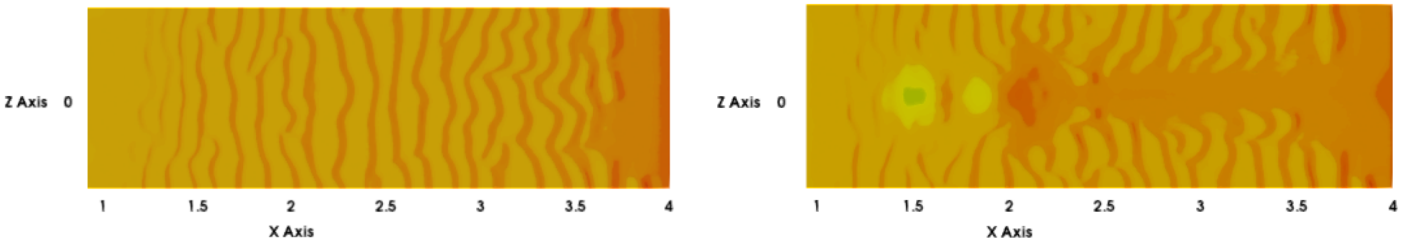

Figure 3: Normalized bed elevations of the bottom in the baseline case (left) and with the turbines 4 turbine diameters apart (right).

References:

[1] C. S. Hill, M. Musa, M. Guala, Interactions between Channel Topography and Hydrokinetic Turbines: Sediment Transport, Turbine Performance, and Wake Characteristics. Renewable Energy, Volume 86, 2016, Pages 409-421.

[2] P. Mycek, B. Gaurier, G. Germain, G. Pinon, E. Rivoalen, Experimental study of the turbulence intensity effects on marine current turbines behaviour. Part I: One single turbine. Renewable Energy, 66, 729-746.

[3] L. Chen, R. Hashim, F. Othman, and S. Motamedi. Experimental study on scour profile of pile-supported horizontal axis tidal current turbine. *Renewable Energy*, 114:744–754, 2017. doi: https://doi.org/10.1016/j.renene.2017.07.026.

[4] M. Musa, C. Hill, and M. Guala. Interaction between hydrokinetic turbine wakes and sediment dynamics: array performance and geomorphic effects under different siting strategies and sediment transport conditions. *Renewable Energy*, 138:738–753, 2019. doi: https://doi.org/10.1016/j.renene.2019.02.009.

[5] J. Chauchat, Z. Cheng, T. Nagel, C. Bonamy, and Hsu T.J. Sedfoam-2.0: a 3-d two- phase flow numerical model for sediment transport, journal of geosci. *Model Dev*, 10: 4367–4392, 2017. doi: https://doi.org/10.5194/gmd-10-4367-2017.

[6] F. Khaled, S. Guillou, Y. Méar, and F. Hadri. Impact of blockage ratio on the transport of sediments in the presence of a hydrokinetic turbine: numerical modelling of the interaction sediments-turbine. *International Journal of Sediment Research*, 2021. doi: https://doi.org/10.1016/j.ijsrc.2021.02.003.

Scour patterns on the bed downstream of a vertical cylinder

Florent Lachaussée,[1] Yann Bertho,[1] Cyprien Morize,[1] Alban Sauret,[2] & Philippe Gondret[1*]

[1] Université Paris-Saclay, CNRS, Laboratoire FAST, 91405 Orsay, France
[2] Department of Mechanical Engineering, University of California, CA 93106 Santa Barbara, USA

* philippe.gondret@universite-paris-saclay.fr

We have investigated experimentally the scour erosion of a non-cohesive granular bed around a vertical cylinder in a small-scale water channel. Two erosion patterns have been found [1]. The classical pattern, which arises from the velocity increase in the vicinity of the cylinder and from the "horseshoe vortex" around it, is shown in Fig. 1(a) and referred here to HS pattern. Another pattern with two elongated holes may be observed downstream of the cylinder as shown in Fig. 1(b). This pattern arises from the wake vortices and is thus referred as WS pattern.

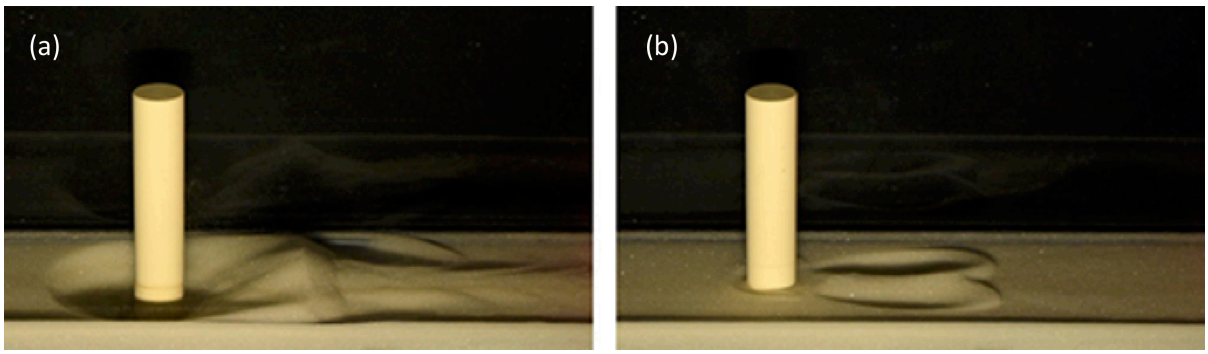

Fig. 1 : Two scour patterns observed on a bed of glass beads of diameter $d \approx 0.3$ mm around a cylinder of diameter $D = 2$ cm : (a) HS pattern for a water velocity $U \approx 0.9\, U_{c,0}$ and (b) WS pattern for $U \approx 0.6\, U_{c,0}$.

The erosion thresholds in terms of water velocity corresponding to these two patterns are significantly below the critical velocity $U_{c,0}$ corresponding to live bed far from the cylinder. Both thresholds depend on the Reynolds number $\mathrm{Re} = UD/\nu$ characterizing the flow around the cylinder of diameter D, but with different scaling laws : $U_{c,HS}/U_{c,0} \approx 1.12\, \mathrm{Re}_D^{-0,19}$ and $U_{c,WS}/U_{c,0} \approx 16\, \mathrm{Re}_D^{-0,66}$. The threshold of the WS pattern is a little smaller than the threshold of the HS pattern but the HS pattern grows much faster and stronger so that the WS pattern is generally hard to observe alone. A laser profilometer has been used to track the bed deformation and PIV measurements have been done to characterize for the water flow. Both patterns can also be observed in the case of non-circular cylinders, with *e.g.* square or triangular cross sections.

[1] F. Lachaussée, Y. Bertho, C. Morize, A. Sauret & P. Gondret Competitive dynamics of two erosion patterns around a cylinder, Phys. Rev. Fluids **3**, 012302 (2018)

Numerical analysis at the particle scale of granular flow hysteresis on an inclined plane

Clovis Lambert[1], Raphael Maurin[1], Marcan Graffin[1], Laurent Lacaze[1], Sylvain Viroulet[1], and Pascal Fede[1]

[1]Institut de Mécanique des Fluides de Toulouse (IMFT), Université de Toulouse, CNRS, Toulouse INP, UPS - Toulouse, France

Granular media are ubiquitous in environmental processes and geophysical phenomenon such as sediment transport, landslides or avalanches. Granular media can be classified into three different regime: solid (quasi-static), liquid (dense flow) and gas (dilute flow). The transition between the motionless solid state and the dense flow state corresponding to the initiation of motion is an important issue for the study of natural hasards such as snow avalanches or landslides. In particular, this transition is subjected to a phenomenon of hysteresis : the angle at which an avalanche starts on an inclined plane is greater than the one at which the flow stops. While this hysteretical behavior has a major influence on avalanche or debris flow propagation, both its description and the underlying basic physical mechanisms still remain open questions.

In this framework, the present work focuses on the fundamental small scale mechanisms related to the hysteresis observed in granular media at the transition between dense granular flow and rest.

Hysterical behaviour has been highlighted in laboratory experiments using either a rotating drum configuration [1], [3] or an inclined plane configuration [5], [4] as the difference of critical angles obtained to initiate and stop granular flow made of monodisperse solid grains. This mechanism has since been often attributed to particle inertia [1], [2]. Yet, more recent works [3], [4] show on that the inter-particle friction is a dominant mechanism in the hysteresis at the expense of the inertia of grains.

To understand this apparent contradiction and the mechanisms at play, the present study focuses on inclined plane simulation at the particle scale. Using a discrete element method modelling the behavior of each particles, flow arrest and avalanche onset are studied by varying the inclination angle of the inclined plane with respect to gravity. Studying the influence of inter-particle friction, it is shown that the inter-particle friction is not the dominant mechanisms responsible for the hysteresis in dry granular flows. Variation of grains inertia are also studied in order to explain the different results on the subject.

[1] S. Courrech du Pont et al. “Granular Avalanches in Fluids”. In: *Phys. Rev. Lett.* 90 (4 Jan. 2003), p. 044301.

[2] E DeGiuli and M Wyart. “Friction law and hysteresis in granular materials”. In: *Proc Natl Acad Sci* 114(35) (2017), pp. 9284–9289.

[3] Hugo Perrin et al. “Interparticle Friction Leads to Nonmonotonic Flow Curves and Hysteresis in Viscous Suspensions”. In: *Phys. Rev. X* 9 (3 Aug. 2019), p. 031027.

[4] Hugo Perrin et al. “Nonlocal Effects Reflect the Jamming Criticality in Frictionless Granular Flows Down Inclines”. In: *Phys. Rev. Lett.* 126 (June 2021), p. 228002.

[5] O. Pouliquen and Y. Forterre. “Friction law for dense granular flows: application to the motion of a mass down a rough inclined plane”. In: *Journal of Fluid Mechanics* 453 (Jan. 2002), pp. 133–151.

Erosion of a model cohesive seabed in wave-current flume

Pierre Lecostey[1], Michael Preioni[2], Guillaume Gomit[1], Sébastien Jarny[1],
Lionel Thomas[1], Damien Pham Van Bang[2]

[1] : Institut Pprime, UPR CNRS 3346, F-86073 Poitiers, France,
[2] : Institut National de la Recherche Scientifique (INRS), Québec, G1K 9A9 QC, Canada,
pierre.lecostey@univ-poitiers.fr

This study proposes a novel approach for studying effect of rheological properties of cohesive seabed on erosion physical processes under waves and currents. Herein we completely control and adjust rheological parameters by using a model sediment or Synthetic Transparent Cohesive Seabed (STCS) and hydrodynamic forcing in small (15x30 cm2 section) laboratory wave flume. STCS, introduced by Pouv (Pouv, et al. 2014) and Tarhini (Tarhini, Bellanger et Jarny 2016), is manufactured from mixture of synthetic polymers and clay having qualitative rheological similarities to natural muddy seabed.

The rheological properties of this laboratory mud can be controlled by diluting the stock preparation. In the wave channel, Planar laser-induced fluorescence (PLIF) with surface detection algorithm have been deployed to visualized STCS dye with fluorescein. Five water height probes are installed above the sediment tank to get wave information. Moreover, the PLIF have been coupled with Particle Image Velocimetry (PIV) to corroborate velocity models based on depth water. The depth water is kept constant to an intermediate depth water according (Le Méhauté 1976). Several waves amplitudes and periods have been tested on different dilution of the model mud. For each case dilution, flowing and oscillating rheological tests have been performed.

Velocity profile obtained by PIV is have been compared to Stocks theory. The correlation between theory and experience allows an estimation of the bottom shear stress as a function of the wave phase. Phase averages analysis allows to establish the relation between wave phase, bottom shear stress and sediment motion. First results highlight a phase shift between the flow velocity and sediments motion as predict by Dalrymple and Liu (Dalrymple et Liu 1978). This phase shift will be analysed for the different wave properties and compare to theoretical models. Some configurations lead to a STCS erosion by blocks. Those observations will be related to wave characteristic and STCS rheological properties.

References

Dalrymple, Robert A., et Philip L.-F. Liu. «Waves over soft muds: A two-layer fluid model.» *American Meteorological Society*, 1978.

Le Méhauté, Bernard. *An introduction to Hydrodynamics & water waves.* 1976.

Mei, Chiang C., et Ko-Fei Liu. «A Bingham-plastic model for a muddy seabed under long waves.» *Journal of Geophysical Research*, 1987.

Pouv, Keang Sè, Besq Anthony, Sylvain S. Guillou, et Erik A. Toorman. «On cohesive sediment erosion: A first experimental study of the local process using transparent model materials.» *Advances in Water Resources*, 2014.

Tarhini, Zaynab, Romain Bellanger, et Sébastien Jarny. «Etude expérimentale d'érosion d'un sédiment cohésif transparent.» *XIV - Journées Nationales Génie Cotier-Génie Civil*, 2016.

Multi-phase simulations of underwater granular collapse in densely packed conditions

Cheng-Hsien Lee[1*] and Yi-Hsuan Kuan[1]

[1] Department of Marine Environment and Engineering, National Sun Yat-sen University, Kaohsiung 80424 Taiwan.

*: Email address for correspondence: kethenlee@gmail.com

Abstract

Underwater granular collapse on an inclined plane was investigated by considering the effects of particle size and initial concentration in densely packed conditions. This study adopted the multi-phase model developed by Lee (2021), which can capture pore pressure feedback (an important mechanism in underwater granular flows). A new set of laboratory experiments were performed to validate the multi-phase model with four different particle sizes (from fine sand to very coarse sand). Generally, the multi-phase model can reproduce all the experimental collapse processes well. Four particle sizes and four initial concentrations were examined numerically. The simulated results reveal that both the volume of the sliding mass in the early stages (initial sliding volume) and the front speed increase monotonically and concavely with increasing particle size. In addition, increasing the initial concentration reduces the initial sliding volume and front speed. The simulated results suggest that the front speed can be expressed as a function of the initial sliding volume. This study also provides a simplified model for determining the initial sliding mass based on a force balance analysis.

Reference:

Lee, C.-H., 2021. Two-phase of submarine granular flows with shear-induced volume change and feedback J. Fluid Mech. 907, A31-1.

Investigation of small scale processes in wave driven sediment transport using Eulerian two-phase large-eddy simulation

Antoine Mathieu[1,2], Zhen Cheng[1], Julien Chauchat[2], Cyrille Bonamy[2], Ali Salimi Tarazouj[1], Tian-Jian Hsu[1]

1. Center for Applied Coastal Research - University of Delaware, Newark DE, USA
2. LEGI - University Grenoble Alpes - Grenoble INP - CNRS, Grenoble, France.

Considering the importance of the cross-shore sand transport on the morphological evolution of beaches, a better understanding of the fine-scale sediment transport mechanisms is an important step toward more accurate predictions of large scale morphodynamic models. In this context, large-eddy simulation of wave-driven sediment transport configurations are reproduced using the Eulerian two-phase flow model sedFoam [1]. Compared with other turbulence-resolving Lagrangian approaches such as fully-resolved direct numerical simulation or the point-particle methodology, the Eulerian representation of the flow for both the disperse and carrier phases allows to overcome the limitations in term of number of particles.

The model is first applied to oscillatory sheet flow configuration with a focus on grain size effects. Numerical results of oscillatory sheet flow configurations from O'Donoghue & Wright (2004) [2] involving medium and fine sand under a sinusoidal flow forcing showed that a complex interplay between bed instabilities, large solid phase Reynolds stresses, turbulence modulation by the presence of the particles and hindered settling contributes to unsteady effects, namely phase-lag effect and enhanced boundary layer thickness for fine sand.

The two-fluid model is then applied to oscillatory sheet flow configurations involving asymmetric and skewed flow forcing from O'Donoghue & Wright [2] and van der A et al. (2010) [3] to study wave shape effects. The comparison between experimental measurements and numerical predictions of the wave-averaged net transport rate shows that the two-fluid model is able to accurately capture the change of sign of the net transport rate for fine sand under skewed waves, signature of the presence of phase-lag effects on the streamwise sediment flux. Simulations results provide further insight into the mechanisms responsible for modifications of the net transport rate for fine sand.

Eventually, the two-fluid model is applied to less energetic flow conditions to study the development of bedforms. Early results from simulations show that the two-fluid model is able to capture the formation of ripples starting from a originally flat bed. Small perturbations of the sediment bed induced by the presence of turbulent flow structures will grow and merge under successive wave periods to generate large ripples. On-going simulations are continued to study ripple scaling and migration rate.

References

[1] J. Chauchat, Z. Cheng, T. Nagel, C. Bonamy, and T.-J. Hsu. Sedfoam-2.0: a 3d two-phase flow numerical model for sediment transport. *Geoscientific Model Development Discussions*, 2017:1–42, 2017.

[2] T. O'Donoghue and S. Wright. Concentrations in oscillatory sheet flow for well sorted and graded sands. *Coastal Engineering*, 50(3):117 – 138, 2004.

[3] D. A. van der A, T. O'Donoghue, and J. S. Ribberink. Measurements of sheet flow transport in acceleration-skewed oscillatory flow and comparison with practical formulations. *Coastal Engineering*, 57(3):331–342, 2010.

Direct numerical simulations reveal the effect of bedload on turbulence dynamics in an oscillatory flow

M. Mazzuoli[1]

[1] *Department of Civil, Chemical and Environmental Engineering (DICCA), University of Genoa, Italy*

THESIS 2022, Les Houches, France, June 6-10 2022

The mechanics of sediment transport under non-breaking monochromatic sea waves has been recently investigated by Mazzuoli et al. (2020) by means of particle-resolved direct numerical simulations (DNS). An oscillatory flow over a horizontal movable bed comprising several layers of monosized quartz spheres was considered. Three different particle sizes in the range of medium sand were employed. For moderate values of the Reynolds number of the bottom boundary layer which fall in the range of the intermittently turbulent regime, Mazzuoli et al. (2020) found that the sediment flow rate associated with rolling/sliding and saltating particles (bedload) can be reasonably estimated considering the oscillatory flow as a sequence of steady states. In the present contribution, the DNS data obtained by Mazzuoli et al. (2020) are further analysed to identify the effects of the sediment particles on turbulence dynamics. The DNS were repeated by keeping the particles fixed at their initial position. Thus, the comparison with the simulations with movable particles allowed us to isolate the effects associated with particle motion. The bottom shear stress was found larger in the fixed particle case, although, above the bottom elevation, the shear stress was enhanced by the presence of moving particles. Moreover, the balance of turbulent kinetic energy (TKE) was computed during the phases of the wave cycle characterised by turbulence (e.g. figure 1). A significant positive TKE production was found to be associated with the moving particles of intermediate size (blue line in figure 1). Finally, the eddy viscosity was evaluated during the wave cycle at different elevations from the bottom. Considerations that can be useful to improve RANS models will be expressed.

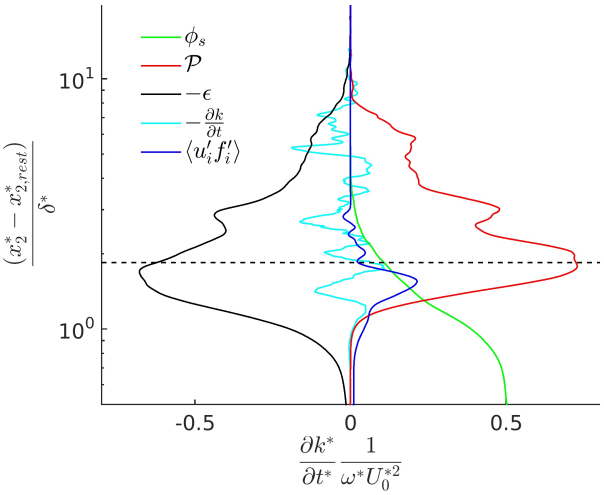

Figure 1: Contributions to the rate of dimensionless TKE, k, averaged over horizontal planes and shown against the dimensionless distance from the resting bed (δ^* denotes the Stokes boundary layer thickness) at the phase when the velocity above the boundary layer is maximum, i.e. equal to U_0^*. The dashed line indicates the mean bottom surface elevation where the solid volume fraction $\phi_s = 0.1$. Particle size $d^*/\delta^* = 0.335$.

References

Mazzuoli, M., Blondeaux, P., Vittori, G., Uhlmann, M., Simeonov, J., and Calantoni, J. (2020). Interface-resolved direct numerical simulations of sediment transport in a turbulent oscillatory boundary layer. *Journal of Fluid Mechanics*, 885.

Field and laboratory investigations into Flow slides.

Peter Nielsen, Xiamei Man & David P Callaghan, School of Civil Engineering, The University of Queensland, Brisbane. p.nielsen@uq.edu.au

Our Coastal group at The University of Queensland is privileged to be close to the World's most dynamic beach at Amity Point, Nth Stradbroke Island 27°23'35"S , 153°26'23"E. Which is about 40km from the University of Queensland campus. This beach experiences regular, flow slide events every two to three weeks at a fixed position, - fixed by an L-shaped rock revetment.

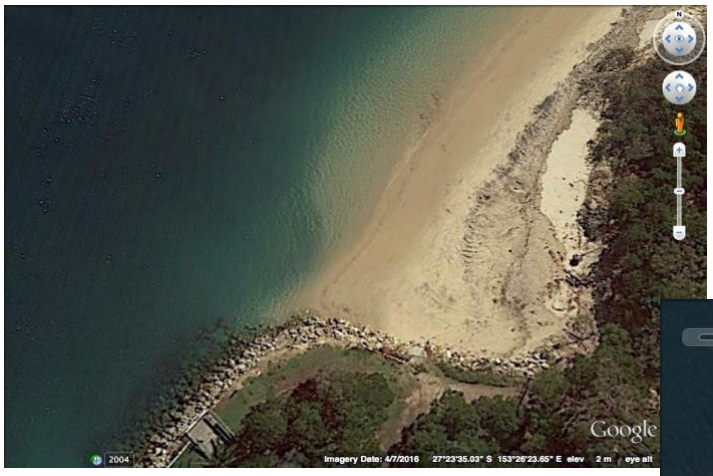

Figure 1a:
Image of the flow slide site in an accreted state taken 4/7-2016.

Figure 1b:
The Amity Point flow slide site shortly after an erosion event.
Image date: 18/8-2014

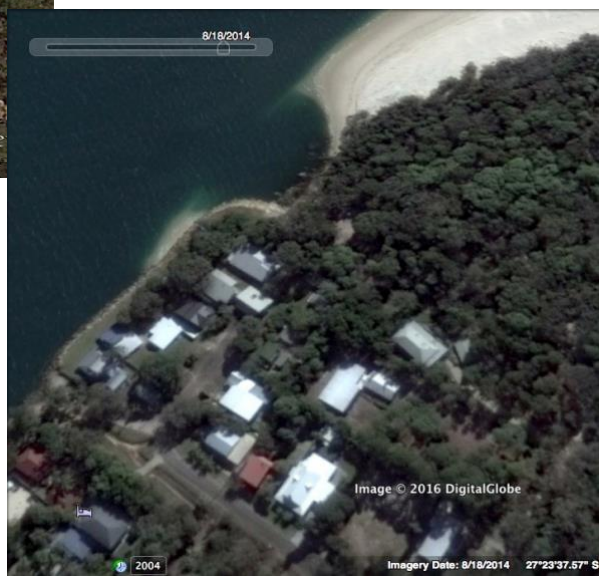

We are in the process of instrumenting the site making use of the unique predictability of regular flow slides at this site. The paper will report progress and hopefully unique field data.

Concurrent with the field work, our group is doing laboratory investigations on these retrogressive breach failures. Key questions addressed by the laboratory work include

- How does the retreat rate of the observed near-vertical submerged sand walls depend on sediment parameters like grain density, grain size, angle of repose ~ friction angle and hydraulic conductivity?
- Does an avalanche on a steep submerged sand face ever create a vertical retreating sand face below the water surface (below the zone of partly saturated sand)? It is well known that a sand dredger removing sand at depth can provoke the formation of a vertical retreating wall.

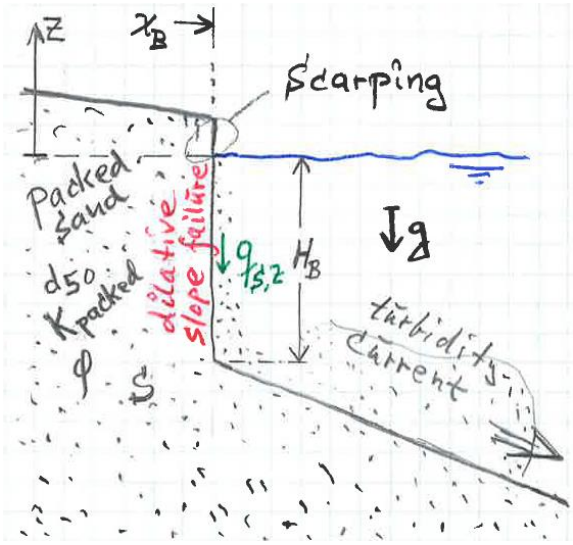

Progress of the laboratory investigations will be reported.

The references below include further details about the unique field site and relevant theory.

REFERENCES

Beinssen, K, D T Neil & D R Mastbergen (2014): Field observations of retrogressive breach failures at two tidal inlets in Queensland Australia, *Australian Geomechanics Vol 49 No 3*, pp 55-63.

Brilli, N, N Stark, P Nielsen, D Callaghan, M Manning & J Culp (2019): Field investigation of two retrogressive breach failures at Amity Point. Poster presented at Coastal Sediments 2019.

Mastbergen, D R, K Beinssen & Y Nedelec (2019): Watching the beach steadily disappearing: The evolution of understanding of retrogressive Breach Failures. *J Marine Science and Eng, Vol 7*, 368.

The effects of dilatancy on submerged granular avalanches and granular column collapses

E. P. Montellà[1], B. Tsai[2] , J. Chauchat [1], B. Chareyre [3] , C. Bonamy [1] , T. J. Hsu[2]

[1]University of Grenoble Alpes, LEGI, G-INP, CNRS, 38000 Grenoble, France

[2]Civil and Environmental Engineering, Center for Applied Coastal Research, University of Delaware,Newark, DE 19711, USA

[3]University of Grenoble Alpes, 3SR, G-INP, CNRS, 38000 Grenoble, France

Abstract

Describing the fluid/grain interaction is a challenging task. Under shear, grains rotate, move and modify the structure of the granular medium. The compression/dilation of the granular medium entails an increase/decrease of the pore fluid pressure, which, in turns, modify the global response of the mixture. In this contribution, we present a two-fluid model accounting for the dilatancy effects and the pore pressure feedback mechanism. The originality of the model is to incorporate dilatancy as an elasto-plastic pressure and not as a modification of the friction coefficient. In order to illustrate the capability of the model, two benchmark cases are proposed: On the one hand, we investigate the initial dynamics of underwater avalanches as function of their initial volume fraction. Experimental data show loose granular layers fully immersed in a fluid flowing down an inclined slope accelerate rapidly, whereas dense granular packings exhibit a time delay before start flowing. This behavior can be explained by a combination of geometrical granular dilatancy and pore pressure feedback on the granular media. On the other hand, we study the dilatancy effects on the collapse of an initially fully saturated granular column. In this case, the increment/reduction of pore fluid pressure, due to the contraction/dilation of the granular medium, changes the effective stress. Therefore, depending on the the initial volume fraction, different collapse dynamics and eventual morphological shapes are expected.

The present model compares favorably with existing experiments for the initiation of underwater granular avalanches and the dynamics of the granular column collapse. Results demonstrate the ability of the model to predict the complex interplay between shear-induced changes of the granular stress and fluid pressure in granular flows.

Keywords— sediment transport, wet granular material, particle/fluid flow

Flow instabilities due to velocity-weakening rheology in shear thickening suspensions

Francisco Rocha[1], Baptiste Darbois Texier[2], Henri Lhuissier[1], Yoël Forterre[1], and Bloen Metzger[1]

[1]Aix-Marseille University, CNRS, IUSTI, Marseille 13453, France
[2]Université Paris-Saclay, Laboratoire FAST, 91405 Orsay, France.

Presenting author's e-mail: francisco.rocha@univ-amu.fr

Shear thickening fluids are granular suspensions whose viscosity drastically increase as they are subjected to higher shear stresses or shear rates. During the past decade, there has been an increasing consensus that this behaviour is a reflect of a transition from a frictionless to a frictional state, mediated by a short-range repulsive force between the constituent particles. One of the consequences of this frictional transition is that the flow rules can be S-shaped, with regions of velocity-weakening (negatively sloped) rheology. In this presentation we will investigate the emergence of instabilities due to this velocity-weakening behaviour in two distinct hydrodynamic configurations. In the first part of the talk we will discuss experiments with a floating layer of shear-thickening fluid in a wide-gap cylindrical Couette cell. Our experiments show that below a critical stress the suspension behaves as a quasi-Newtonian fluid, and above this critical value the flow becomes unsteady and marked by periodic jamming fronts that propagate through the material. For the second part, we will concentrate on the gravity-driven flow of a shear thickening suspension down an inclined plane. For solids volume fraction whose flow rules display velocity-weakening behaviour, the flow becomes unstable, triggering surface waves at a critical Reynolds number, much smaller than the threshold for the emergence of Kapitza waves. By applying a depth-integrated model, we show that the instability arises not from inertia, but from the coupling between free-surface deformations and the velocity-weakening rheology. This mechanism, which gives rise to a new class of kinematic waves without inertia, is very generic and could also be extended to other complex fluids displaying a velocity-weakening rheology (e.g. granular materials, geomaterials, etc).

Friday, 22th of April 2022

Modelling the vertical structure of turbulent flows over still rough sediment beds

Gauthier Rousseau[1]

[1] Institute of Hydraulic Engineering and Water Resources Management, TU Wien, Karlsplatz 13, 1040, Vienna, Austria

Description

In the absence of sediment transport, the two-phase problem of flows in river is simplified: the fluid flows over a still solid phase, i.e. a rough permeable sediment bed. There is an apparent lack of experimental data and attempts to validate bi-phasic modelling tools in this immobile limit configuration. Yet, this validation step seems critical in order to predict flows with no transport or flows with low sediment transport rates (i.e. when the solid phase flux has a negligible role on dynamics). In order to shed light on this problem, PIV measurements on turbulent flows adjacent to a macro rough permeable bed made up of coarse particles have been collected using a refracive index matched technique. Space-time averaged quantities over a representative elementary volume allows recovering mesoscopic *double-averaged* profiles (turbulent and dispersive stresses). Averaging quantities over a sufficiently large domain is crucial in order to adequately test bi-phasic models working at the mesoscale.

I compare the collected experimental profile to bi-phasic models employing mixing length approaches and more elaborated $k-\epsilon$ or $k-\omega$ approaches adapted for the prediction of 3D scenarios. Because discrepancies are found between experimental profiles and modelled profile using previously developed closures, a mixing length closure for the shear stress has been developed taking into account damping and dispersive effect.

A good agreement is shown between the model and classic flow resistance laws employed for river studies. The model contrasts with existing boundary-layer models which assume a discontinuous porosity profile at bed interface (be the bed permeable or impermeable).

Graphical abstract

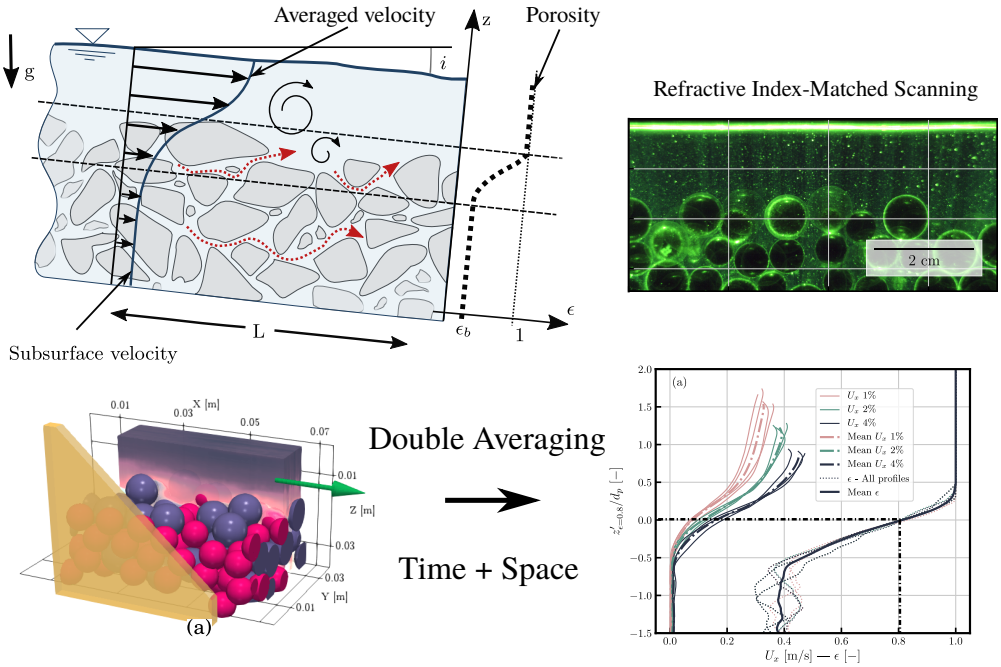

AN INVESTIGATION OF WAVE-SHAPE EFFECT ON SAND RIPPLE DYNAMICS USING SEDFOAM

Ali Salimi-Tarazouj*, Tian Jian Hsu*, Peter Traykovski**, Julien Chauchat***
* Center of Applied Coastal Research (CACR), Civil and Environmental Engineering Department, University of Delaware
**Applied Ocean Physics & Engineering, Woods Hole Oceanographic Institution
*** University of Grenoble Alpes, LEGI, F-38000 Grenoble, France

INTRODUCTION

Sand ripples can form and migrate during moderate wave-energy conditions in the shoaling and surf zones due to the interaction of seabed and near-bed oscillatory flows which contain higher harmonics (e.g., orbital velocity skewness and/or asymmetry). The importance of ripples arises from their effect on the seabed roughness and boundary layer hydrodynamics which controls the net onshore/offshore sediment transport. The dynamic behavior of sand ripples affects the wave attenuation, acoustical properties of the seafloor, and it is an important factor for the object burial process. Understanding the different sediment fluxes above these migrating ripples driven by skewed and/or asymmetric oscillatory flows is the main objective of the present study. We utilize an Eulerian two-phase model, SedFOAM, to investigate the wave-shape effect on the sand ripple dynamics. Model results reveal the mechanism on how the different mechanisms drive onshore ripple migrations.

MODEL DESCRIPTION AND FORMULATION

The SedFOAM was developed under the open-source CFD toolbox OpenFOAM (Chauchat et al. 2017). With closures of particle stresses and fluid-particle interactions, the model can resolve processes in the concentrated region of sediment transport and hence does not require conventional bedload/suspended load assumptions. Assuming that there is no mass transfer between the two phases, the mass conservation equations for fluid phase and sediment phase can be written as,

$$\frac{\partial \alpha}{\partial t} + \frac{\partial \alpha u_i^a}{\partial x_i} = 0,$$
$$\frac{\partial \beta}{\partial t} + \frac{\partial \beta u_i^b}{\partial x_i} = 0,$$

α and β are particles and fluid volume concentrations ($\alpha + \beta = 1$) and u_i^a and u_i^b are particle and fluid phase velocities, respectively. The momentum equations for fluid and particle phases are written as:

$$\frac{\partial \rho^a \alpha u_i^a}{\partial t} + \frac{\partial \rho^a \alpha u_i^a u_j^a}{\partial x_j} = -\alpha \frac{\partial p}{\partial x_i} + \alpha f_i - \frac{\partial \widetilde{p}^a}{\partial x_i} + \frac{\partial \tau_{ij}^a}{\partial x_j} + \alpha \rho^a g_i + \alpha f_i + \alpha\beta K (u_i^b - u_i^a) - S_{US}\ \beta K \nu_t^b \frac{\partial \alpha}{\partial x_i},$$

$$\frac{\partial \rho^b \beta u_i^b}{\partial t} + \frac{\partial \rho^b \beta u_i^b u_j^b}{\partial x_j} = -\beta \frac{\partial p}{\partial x_i} + \beta f_i + \frac{\partial \tau_{ij}^b}{\partial x_j} + \beta \rho^b g_i + \beta f_i - \alpha\beta K (u_i^b - u_i^a) + S_{US}\ \beta K \nu_t^b \frac{\partial \alpha}{\partial x_i},$$

ρ^a and ρ^b are particle and fluid density, respectively, f_i is external forces driving the oscillatory flow and g_i represents gravity acceleration. Viscous and Reynolds stresses for the fluid phase are combined in τ_{ij}^b. In this study, the standard $k-\epsilon$ model is used as turbulence closure for Reynolds stresses. Finally, τ_{ij}^a and $\tilde{p}_i^a$ are particle shear and normal stresses. Particle stresses due to collisions and frictions are modeled by the kinetic theory and empirical formulae. The last two terms in momentum equations are momentum exchange between two phases, modeled as mean drag force and turbulent suspension.

MODEL VALIDATION

Model verifications were performed for full-scale water tunnel experiments conducted by Yuan and Wang (2019) for orbital ripples driven by asymmetric (forward-leaning) oscillatory flow. Modeled ripple geometry, flow velocity, net sediment transport rate, and ripple migration speed are compared against the measured data with good agreements. By keeping the same sand grain size D_{50} = 0.51mm, flow period T=6.25sec, and mobility number $\psi = 42$, the identical initial ripples are driven by a skewed (2nd order Stokes) and a combined skewed-asymmetric flow for better understanding of the wave-shape effect on different sediment fluxes over the migrating ripples.

RESULTS

We initialized the model with a sinusoidal ripple bed consisting of three ripples with periodic lateral boundaries. After 10 flow periods, the ripples reach equilibrium and become more realistic in shape (Figure-1A). Model results showed that the so-called "phase-lag effect" associated with skewed, or asymmetric flows drives completely opposite suspended load fluxes over ripples (see the left panel in Figure-1B). However, a greater net near-bed load (onshore directed) forces a larger onshore migration rate under asymmetric flow, compared to skewed flow (see the right panel in Figure-1B); under the skewed case, the onshore migration rate is limited by the stronger offshore sediment flux due to the lee vortex returning flow. Consequently, the net transport rate is onshore (offshore) directed under asymmetric (skewed) flow. In the combined skewed-asymmetric case, the near-bed load and migration rate are even larger than the asymmetric case. Moreover, the offshore-directed suspended load is much weaker compared to the skewed case due to a competition between negative (due to skewness) and positive (due to asymmetry) phase-lag effects. As a result, the net transport rate is slightly smaller than in the purely asymmetric case.

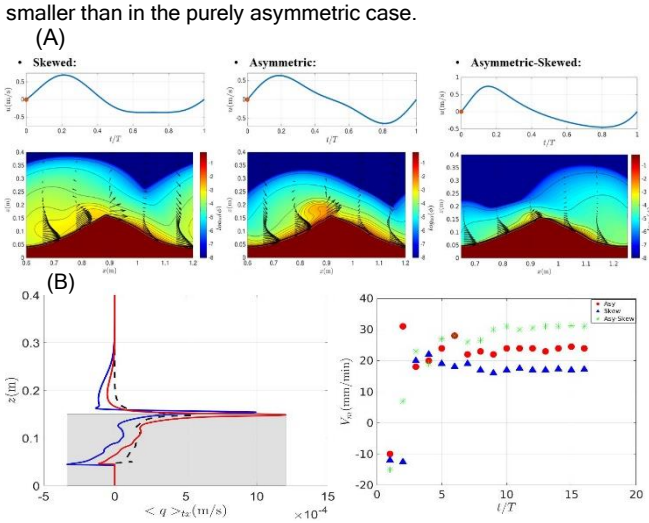

Figure 1: (A) Snapshot of equilibrium ripple bed after 10 wave periods (colorbar represent concentration) and velocity field (vectors) driven by different the free stream velocity time series (top panels). (B) left panel: wave period and ripple-averaged sediment flux for asymmetric flow (black-dashed), skewed flow (blue-solid), and combined flow (red-solid); right panel: ripple migration rate for asymmetric (red), skewed (blue), and combined flows (green).

REFERENCES

- Chauchat et. al., (2017). SedFoam-2.0: a 3-D two-phase flow numerical model for sediment transport, 105194, 4367-4392. https://doi.org/10.5194/gmd-10-4367-2017.
- Yuan and Wang, An experimental investigation of asymmetric oscillatory flow over vortex ripples (under review), J. Geophys. Res. (2019).
- Salimi-Tarazouj et. al., (2021a). A numerical study of onshore ripple migration using a Eulerian two-phase model. JGR-Oceans.

Three-dimensional process of laterally unconfined hyperpycnal current plunging

H. Shi[1], M. E. Negretti[2], J. Chauchat[2], K. Blanckaert[3], U. Lemmin[1], D. A. Barry[1]

[1]Ecological Engineering Laboratory (ECOL), Environmental Engineering Institute (IIE), Faculty of Architecture, Civil and Environmental Engineering (ENAC), École Polytechnique Fédérale de Lausanne (EPFL), Lausanne, Switzerland
[2]Université Grenoble Alpes, CNRS, Grenoble INP, LEGI UMR 5519, Grenoble, France
[3]Research Unit Hydraulic Engineering, Institute of Hydraulic Engineering and Water Resources Management, Technische Universität Wien, Vienna, Austria

Submitted to Thesis 2022, 5th symposium on particulate geophysical flows

Abstract

Negatively buoyant river flow entering into a lake usually develops a hyperpycnal current at the river mouth that plunges toward the lake bottom and then turns into an underflow. The excess density of the river flow usually arises from lower temperature or suspended sediment load. In several previous studies, river plunging was examined in 2D side-constrained channels. However, recent field measurements and large-scale surface imagery of the sediment-laden Rhône River plume entering Lake Geneva make evident the three-dimensionality of laterally unconfined plunging. That is to say, the current converges near the surface forming a triangular shape and spreads laterally near the bottom. To improve understanding of this 3D process, a laboratory experiment was performed and an LES numerical model established using salinity to control the density difference. The results show that while the hyperpycnal current flows out into the receiving water body, it also sinks laterally at the two sides due to the density difference between the current and ambient water. Thus, in the lateral direction, the current behaves like a lock-exchange density current, generating a transversal velocity from the sides to the middle on the surface and in the opposite direction near the bottom. The superposition of the longitudinal and transversal velocity vectors results in a flow pattern that produces a triangular velocity (and density) contour on the surface and causes the near-bottom cross-section to be much wider than the surface triangle and also wider than the inflow channel. In contrast to 2D hyperpycnal currents, which plunge at one single longitudinal distance, this 3D current progressively plunges at its surface triangular edge. The numerical model results are also compared with the surface images of the Rhône River mouth, showing acceptable applicability in estimating the surface triangular shape in the field, although the deposition of sediment was not considered.

Erosion by an oscillating disc in the vicinity of a granular bed

Joanne Steiner[1*], Cyprien Morize[1], Alban Sauret [2] and Philippe Gondret[1]

[1] Laboratoire FAST, CNRS, Université Paris-Saclay, F-91405 Orsay, France
[2] Department of Mechanical Engineering, University of California, CA 93106 Santa Barbara, USA
*email : joanne.steiner@universite-paris-saclay.fr

Flatfish, such as flounders, bury themselves in the sand to hide from predators. They are able to hide very quickly by oscillating their fins close to the seabed leading to the suspension of sand, which then fall onto their bodies. Our experimental set-up aims at reproducing while simplifying this natural behaviour. A rigid disc of diameter D and at an average distance H from a flat granular bed is set to oscillate at a frequency f (or period T) and an amplitude A such that the position of the disc is given by $H + A\sin(2\pi ft)$.

We study experimentally the erosion thresholds in the simple case of a half-oscillation, which means that the disc only moves downwards or upwards with smooth acceleration and deceleration. The influence of the relevant parameters, i.e. A, D and H as well as the initial position of the disc, on the erosion threshold is systematically characterized by finding the critical half-period $\tau_c = T_c/2$ below which beads are set into motion. In the range of parameters considered in this study, the roll-up of the shear layer produced at the edge of the disc generates a vortex ring that is one of the main mechanisms responsible for the erosion of the granular bed. The key features of the vortex generated are then characterized by PIV (Particle Image Velocimetry) and related to the parameters of the experiments. The characterization of the fluid flow generated provides a better understanding of the erosion thresholds.

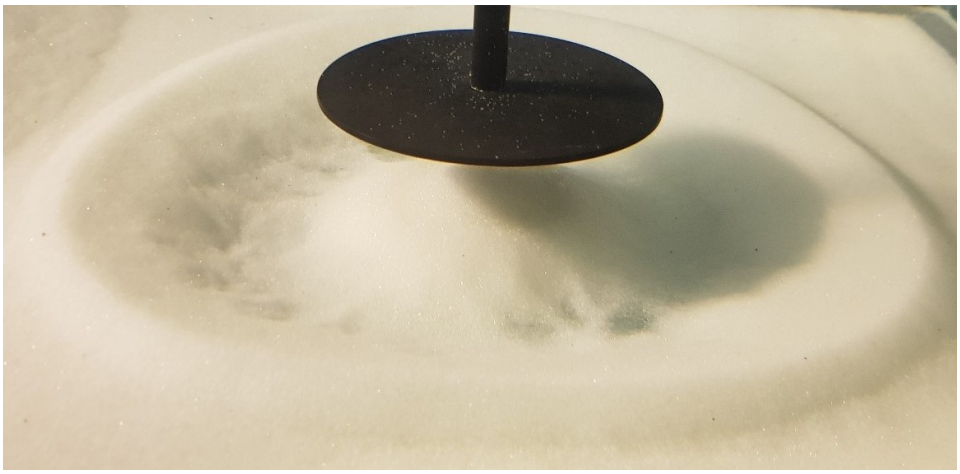

Figure 1: Circular erosion pattern created by the oscillating disc in water above a granular bed of glass beads of diameter $d_p = 0.3$ mm. The experimental parameters are here $D = 10$ cm, $A = 1.4$ cm, $f = 2.3$ Hz.

Effects of particle volume and shape on saltation motion of single particle in a turbulent flow over roughened bed

Yuya Takakuwa, Assistant Professor, Research and Development Initiative, Chuo University, Japan.
E-mail: ytakakuwa099@g.chuo-u.ac.jp
Shoji Fukuoka, Professor, same as above, E-mail: sfuku@tamacc.chuo-u.ac.jp

Key Words: Non-spherical particle, Instantaneous particle velocity, Fluid force and contact force, Transport manner

To clarify bed variation mechanism in gravel-bed rivers and the abrasion mechanism of sediment bypass tunnels of dams, it is necessary to evaluate the three-dimensional motion of particles with various volumes and shapes in turbulent flows over complex bed roughness. Fukuda and Fukuoka (2019) have developed the APM method to solve the mechanism of debris flows.

In this paper, numerical simulations of saltation of single particles with various volumes (d = 75, 105, 135mm) and shapes shown in Fig.1 (Natural gravel: A-Disk type, B-Massive and symmetric, C-Massive and asymmetric. Artificial particle: D-Sphere) were conducted using the APM method. Effects of volume and shape on the particle velocity are investigated by computing the particle orientation and fluid forces and contact forces acting on particle.

Probability density distributions of the instantaneous streamwise particle velocity "u_p" differ greatly depending on volumes and shapes. The particle (d = 75mm) velocity u_p varied from 0.6 to 1.05 times the depth-averaged flow velocity "$\overline{U}_c$" in the channel center, regardless of particle shape. As shown in Fig.2(a) the particle (d = 105mm) velocity u_p of the sphere changed from 0.75 to 1.02 times as much as $\overline{U}_c$, while the u_p of the disk-shaped particle (d = 105mm) from 0.62 to 1.05 times of $\overline{U}_c$. The effect of particle shapes becomes remarkable when the ratio of the particle size to the bottom roughness becomes large. In addition, as shown in Fig.2(b), the maximum value of the transverse component "v_p" of sphere was about ±0.4m/s, while that of non-spherical particles was ±0.7m/s. Non-spherical particles are seen to move in three-dimensional manner.

After a particle collides with the channel bottom, the projected area becomes large with respect to the flow, and then a particle tends to increase its speed. Therefore, non-spherical particles with large dimensionless maximum projected area (Maximum projected area / projected area of sphere of equivalent volume) were more likely to accelerate. Correspondingly, the contact force also increased, and the variation in u_p increased.

Our study showed the importance of the instantaneous particle motion and showed possibilities that the understanding of sediment transports in gravel-bed rivers could be improved.

Reference

1) Fukuda and Fukuoka (2019). *Advances in Water Research*, 129, 297-310.

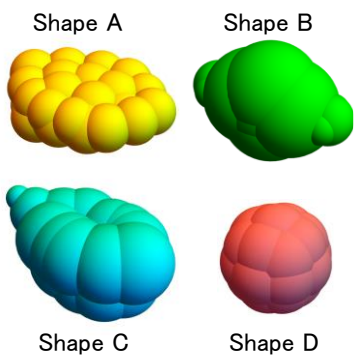

Fig.1 Particle shape.

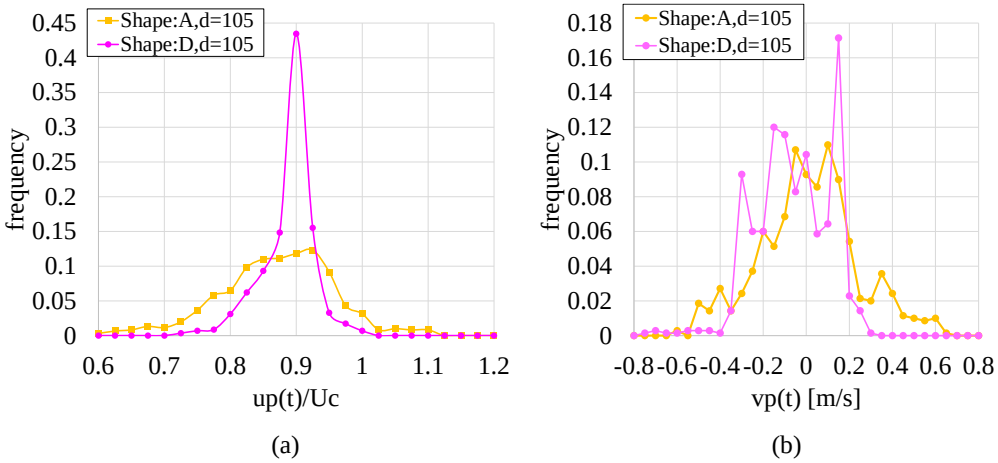

Fig.2 Probability density distributions for up (a) and vp (b) (d=105mm)

Accounting for energy dissipation by particle motion in a suspension in sediment transport models at different scales

Erik A. Toorman (erik.toorman@kuleuven.be)
Hydraulics & Geotechnics Section, Dept. of Civil Engineering, KU Leuven, Belgium

Ever since the observation that it remains impossible to properly resolve velocity and suspended sediment concentration profiles with CFD models, the author has been investigating this problem at different scales by analyzing experimental data, theoretical investigations and numerical model development. Eventually, this has led to the development of a research strategy which has been converted into a research proposal submitted to the Flemish Science Foundation (FWO). The corresponding 4-year fundamental research project, entitled "*Quantification of hydrodynamic energy losses by particle transport in the inner boundary layer of suspension flows with high particle concentrations*" has been awarded by the FWO and started in January 2022.

The main research hypothesis is that the proper inclusion of energy consumption by particle transport in suspension flow CFD, in particular by bedload in the inner boundary layer (IBL), will allow a much more accurate calculation of the hydrodynamics, free surface wave propagation and morphodynamics in environments with erodible beds.

The following specific fundamental research question will be addressed by this project: *How much energy from currents and waves is consumed by particle transport in the inner boundary layer of turbulent free-surface flow?*

This is converted into the definition of the following major objectives:

1. Development of a high-resolution model for particle transport in the inner boundary layer of a turbulent free-surface flow with a new low-Reynolds turbulence model;
2. Development of new bedload (or IBL sediment) transport models for non-cohesive (sand) and cohesive (mud) sediments for implementation in large-scale morphodynamic models;
3. Development of new analytical wall functions to construct new near-bed boundary conditions for both fine and coarse resolution modelling of sediment-laden flows;
4. Development of subgrid scale process models for energy dissipation accounting for the impact of IBL sediment transport on (a) the flow and (b) the wave energy in coastal engineering software;
5. Improvement of the front propagation calculation method for inundation flows on intertidal areas (including beaches).

The main challenge will be the bridging of multiple scales: from the turbulence in the inner boundary layer, to the scale of morphodynamic changes in coastal areas over periods of a one day storm or longer. The IBL process models will also generate new bed boundary conditions for the flow and suspension transport in the water column. The high-resolution model(s) will first be implemented in an in-house developed 1DV model (Matlab code) and validated with available experimental data from a.o. Cellino (1998) and Guta *et al.* (2022). The IBL process models for large-scale applications are created by parameterization of data generated by the high-resolution multi-phase Mixt3SedFOAM model (Ouda & Toorman, 2019), which is used as a numerical laboratory, allowing to generate much more data than possible in a physical experiment (as in Zhang *et al.*, 2022). The new parameterizations will be implemented in TELEMAC models for the Belgian Coast and the Scheldt Estuary and validated, in collaboration with Flanders Hydraulics Research.

Acknowledgement: This project is funded by the Flemish Science Foundation (FWO Vlaanderen) under contract G084922N.

References

Cellino M. (1998). *Experimental study of suspension flow in open channels*. Ph.D. thesis, Dept. of Civil Engineering Ecole Polytechnique Fédérale de Lausanne, Lausanne, Switzerland.

Guta H., Hurther D., Chauchat J. (2022). Bed-load effects on turbulent suspension properties in heavy particle sheet-flows. *J. Hydraulic Engineering* (in press).

Ouda M., Toorman E.A. (2019). Development of a new multiphase sediment transport model for free surface flows. *Int. J. of Multiphase Flow*, 117(8): 81-102.

Zhang Q., Ouda M., Monbaliu J., Toorman E.A. (2022). Sheet flow under progressive waves and its subsequent enhanced wave bottom dissipation: a numerical study. *Coastal Engineering* (in press).

An Eulerian two-phase model investigation on wave-induced scour around a vertical circular cylinder

Benjamin Tsai[1*], Antoine Mathieu[2], Tian-Jian Hsu[1], Julien Chauchat[2]
btsai@udel.edu antoine.mathieu@univ-grenoble-alpes.fr thsu@udel.edu julien.chauchat@univ-grenoble-alpes.fr
[1] *Center for Applied Coastal Research, Department of Civil and Environmental Engineering, University of Delaware, Newark, DE 19716, USA*
[2] *LEGI, University of Grenoble Alpes, G-INP, CNRS, 38000 Grenoble, France*
[*] *Corresponding author*

Abstract

A three-dimensional Eulerian-Eulerian two-phase flow solver, SedFoam has been developed for various sediment transport applications. It has been proven to successfully model sediment transport under oscillatory flows in sheet flow and bedforms modes with a Reynolds-averaged Navier–Stokes (RANS) formulation (Cheng et al., 2017; Salimi-Tarazouj et al., 2021). Recently, the large-eddy simulation (LES) approach has been added into SedFoam as an alternative turbulent closure option (Cheng et al., 2018; Mathieu et al., 2021). In this study, we apply SedFoam on three-dimensional wave-induced local scour around a single vertical circular cylinder. We have chosen to simulate two experimental tests (Sumer et al., 2013) with Keulegan-Carpenter (KC) numbers 10 and 20. Kinetic theory is adopted and k-ω turbulent model is chosen to resolve vortex shedding features around the vertical cylinder. The numerical results are shown in Figure 1. SedFoam is able to capture vortex shedding and scour development (see Figure 1(a)). The model well predicts the scour development in the early stage of the high KC number case (KC = 20, Figure 1(c)). However, for the low KC number case (KC = 10, Figure 1(b)), the scour development is over-predicted. The model also tends to under-estimates the equilibrium scour depth in both cases which may be cause by either turbulent closure or sediment stress closure. Consequently, LES will be carried out for these two benchmark cases and inter-turbulent model comparison between RANS and LES will be further discussed. Furthermore, a widely used Soil Plasticity Theory will be implemented to improve sediment stress behavior. The updated results will be presented in the symposium.

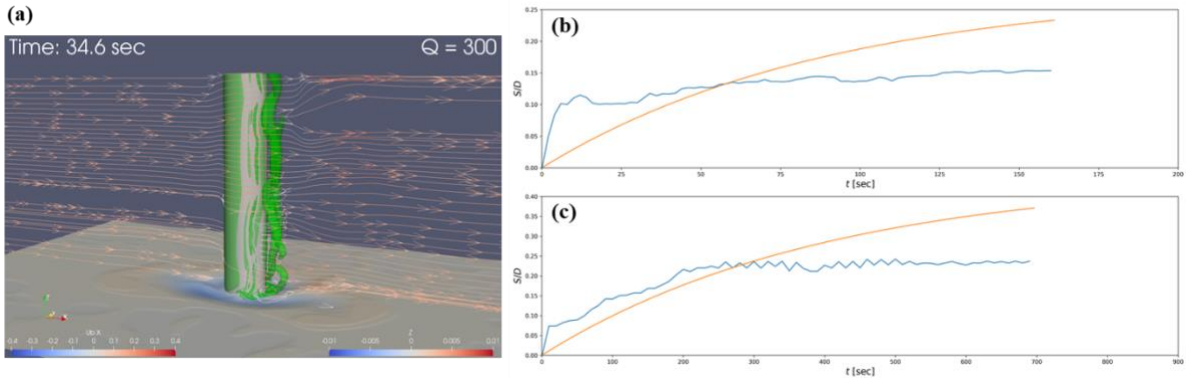

Figure 1. (a) Scour hole and turbulent coherent structures and the comparison of temporal development of maximum scour depth between numerical results (blue lines) and fitting curve from experimental results (orange lines) with (b) KC = 10 and (c) KC = 20.

References

Cheng, Z., Hsu, T.-J., & Calantoni, J. (2017). SedFoam: A multi-dimensional Eulerian two-phase model for sediment transport and its application to momentary bed failure. *Coastal Engineering*, *119*, 32–50. https://doi.org/10.1016/j.coastaleng.2016.08.007

Cheng, Z., Hsu, T.-J., & Chauchat, J. (2018). An Eulerian two-phase model for steady sheet flow using large-eddy simulation methodology. *Advances in Water Resources*, *111*, 205–223. https://doi.org/10.1016/j.advwatres.2017.11.016

Mathieu, A., Chauchat, J., Bonamy, C., Balarac, G., & Hsu, T.-J. (2021). A finite-size correction model for two-fluid large-eddy simulation of particle-laden boundary layer flow. *Journal of Fluid Mechanics*, *913*. https://doi.org/10.1017/jfm.2021.4

Salimi-Tarazouj, A., Hsu, T.-J., Traykovski, P., Cheng, Z., & Chauchat, J. (2021). A Numerical Study of Onshore Ripple Migration Using a Eulerian Two-phase Model. *Journal of Geophysical Research: Oceans*, *126*(2), e2020JC016773. https://doi.org/10.1029/2020JC016773

Sumer, B. M., Petersen, T. U., Locatelli, L., Fredsøe, J., Musumeci, R. E., & Foti, E. (2013). Backfilling of a Scour Hole around a Pile in Waves and Current. *Journal of Waterway, Port, Coastal, and Ocean Engineering*, *139*(1), 9–23. https://doi.org/10.1061/(ASCE)WW.1943-5460.0000161

An Available Porosity Concept for a Multiphase Eulerian Formulation on Mixed-Size Grain Sediment Problems

Tatsuhiko Uchida

Graduate School of Advanced Science and Engineering, Hiroshima University, 1-4-1 Kagamiyama, Higashi-Hiroshima City, Hiroshima 739-8527, Japan. Email: utida@hiroshima-u.ac.jp

Two-phase model has contributed to complicated sediment transport problems, which are difficult to be solved with previous sediment transport model, employing solving momentum equations of fluid and sediment particles to take into account of those interactions. For geophysical flow problems such as river flow, the existence of Grain Size Distribution (GSD) further complicates the sediment transport problem. In fact, while the active layer concept has been applied to sediment transport problems in mixed-grained river beds in the past half century, the problems of porosity and exchange layer thickness remain unsolved. However, it is not appropriate to consider the riverbed height (or sediment volume including porosity) as a conservative quantity when considering sediment supply by slope failure, dams, and sediment deposition in river channels, since the porosity of a riverbed changes due to the sediment sorting effect of flow. In addition, the active layer thickness, which is known as an important parameter that controls the sensitivity of GSD calculations, has been determined empirically based on the representative grain size such as the maximum grain size. Although many attempts have been made to solve these problems related to sediment transport with mixed particle sizes, the problems of porosity and exchange layer thickness seem to remain unresolved. On the other hand, the discrete element method (DEM), which analyzes individual particles in a Lagrangian manner, has been focused on as a tool to solve the unsolved problems of conventional sediment transport with GSD. While the application of DEM has been limited to simple conditions with a relatively narrow ranges of GSD for computational cost, it is important to note that the problems of the active layer does not appear in DEM. Because the Lagrangian method for DEM is a kind of discretization method, it should be possible to solve the problems with an Eulerian method without introducing active layer and be coupled with existing fluid phase models for sediment transport analysis.

The authors [1] developed an Eulerian model for formulation sediment deposition problems with GSD by proposing an available porosity (AP) defining a space for each particle class in the mixed grain size where the particles can enter among the coarser particles, instead of introducing an artificial layer for the continuity equations. This model is able to take into account changes in porosity of mixed-grained sediment due to GSD and increase/decrease of sediment volume due to water flow (classification/mixing). However, the erosion process has not been discussed enough. In this study, the relationship between the present Eulerian model and the conventional models of based on the active layer concept, essential issues such as why the exchange layer is not necessary in DEM is clarified. Decreasing mechanism of coarse sediment height in erosion processes induced by fine sediment transport were investigated experimentally. The process was also formulated based on AP concept, considering the constrain condition, in which the coarser particles cannot across the deposition height of the finer particles. The variation in deposition height in erosion stage was reproduced by the present theory.

References

[1] Uchida, T., Kawahara, Y., Hayashi, Y., and Tateishi, A. (2020) Eulerian deposition model for sediment mixture in gravel-bed rivers with broad particle size distributions, J. Hydraul. Eng., Vol 146(10).

Numerical investigation of scour erosion around free surface piercing vertical cylinder

Wei Zhang[1], Miguel Uh Zapata[2,3], Damien Pham Van Bang[3], Kim Dan Nguyen[4]

[1]*Department of Civil Engineering, Xi'an Jiaotong-Liverpool University, Suzhou,215123, CHINA*

[2] *Conacyt, Centro de Investigación en Matemáticas A.C., CIMAT Unidad Mérida, Sierra Papacal, CP, Mérida, Yucatan 97302, MEXICO*

[3] *Laboratory for Hydraulics and Environment (LHE), Institut National de la Recherche Scientifique, Université du Québec, 490 rue de la Couronne, G1K 9A9 Québec (QC), CANADA*

[4] *Laboratory for Hydraulic Saint-Venant (LHSV, ENPC-EDF R&D-Cerema), Université Paris-Est, 6 quai Watier, BP 49, 78401 Chatou Cedex, FRANCE*

E-mail: wei.zhang01@xjtlu.edu.cn

Scour erosion studies during high-speed flows are essential for risk assessments of civil structures under climate change effects, such as bridge piers or offshore Aeolian piles. During those extreme flows, a high Froude number is expected. The impact of the free surface may significantly affect flow properties near a pile structure [1]. To more detail the indirect effect of free surface on bed morphodynamics, we perform a numerical simulation with relatively high Froude number and low water depth to cylinder diameter ratios. A three-dimensional unstructured finite volume method is used with a projection method to decouple the pressure and velocity in N-S equations. The σ-transformation [2] is applied to the vertical coordinate to fit the computing mesh in describing the evolution of the free surface. Velocity profile, surface elevation and vortex shedding (figure 1) in the vicinity of the cylinder are present. Comparisons between free surface and rigid surface results are also carried out.

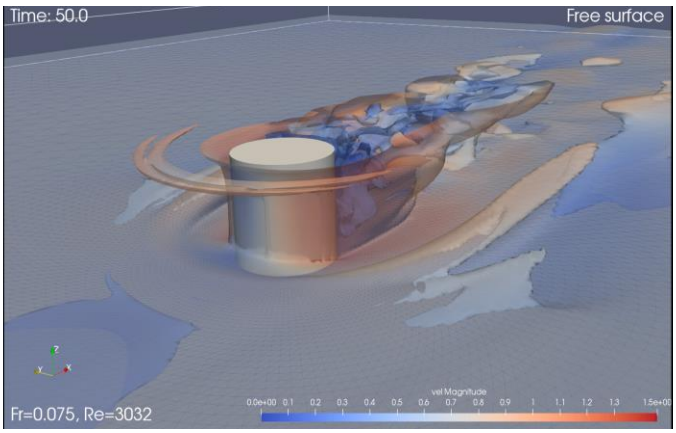

Figure 1. Simulation result of a bow wave around a cylinder at a certain instant.

References :

[1] Johnson KR, FC Ting. Measurements of water surface profile and velocity field at a circular pier. *Journal of engineering mechanics*, vol. 129, pp. 502–513, 2019.

[2] Wei Zhang, Miguel Uh Zapata, Xin Bai, Damien Pham-Van-Bang, Kim Dan Nguyen, 3D simulation of horseshoes vortex and local scours around a vertical cylinder using an unstructured finite-volume technique, *International Journal of sediment research*, vol. 35, pp. 295–306, 2019.

Three-dimensional unstructured finite-volume two-phase model for sediment release

Miguel Uh Zapata[1,2], Wei Zhang[3], Damien Pham Van Bang[2], Kim Dan Nguyen[4]

[1] *Conacyt, Centro de Investigación en Matemáticas A.C., CIMAT Unidad Mérida, Sierra Papacal, CP, Mérida, Yucatan 97302, MEXICO, angeluh@cimat.mx*

[2] *Laboratory for Hydraulics and Environment (LHE), Institut National de la Recherche Scientifique, Université du Québec, 490 rue de la Couronne, G1K 9A9 Québec (QC), CANADA*

[3]*Department of Civil Engineering, Xi'an Jiaotong-Liverpool University, Suzhou,215123, CHINA*

[4] *Laboratory for Hydraulic Saint-Venant (LHSV, ENPC-EDF R&D-Cerema), Université Paris-Est, 6 quai Watier, BP 49, 78401 Chatou Cedex, FRANCE*

In this work, a fully algorithm for a three-dimensional two-phase Eulerian approach is presented and applied for the numerical solution of two-phase fluid-solid problems. The importance of the two-phase flow model relies upon the correct simulation of specific problems in which a single-phase model fails. Moreover, a three-dimensional model is required to fully understand the problem without the physical limitations of a two-dimensional formulation. This modelling framework is particularly well-suited to such a test case since fluid and solid phase velocities differ in amplitude and direction. In this model, the computing domain is extended to the true non-erodible bed so that no extra-consolidation and sedimentation bed model is needed. The continuity and motion equations are solved for both fluid and solid phases. Fluid flows are free surface and considered as non-hydrostatic. The main physical processes for sediment transport such as fluid-solid particles, particle–particle interactions, particle–wall collision, and fluid-bottom exchanges are integrated into the equations of motion and treated as momentum exchanges between phases. The numerical method is designed by a three-dimensional unstructured finite-volume technique. A projection technique is applied to calculate the pressure and velocity for each phase. The σ-transformation is applied to the vertical coordinate in order to fit the computing mesh to the free surface evolution. Finally, comparisons between three dimensional numerical and experiments results are carried out on sediment release, see Figure 1.

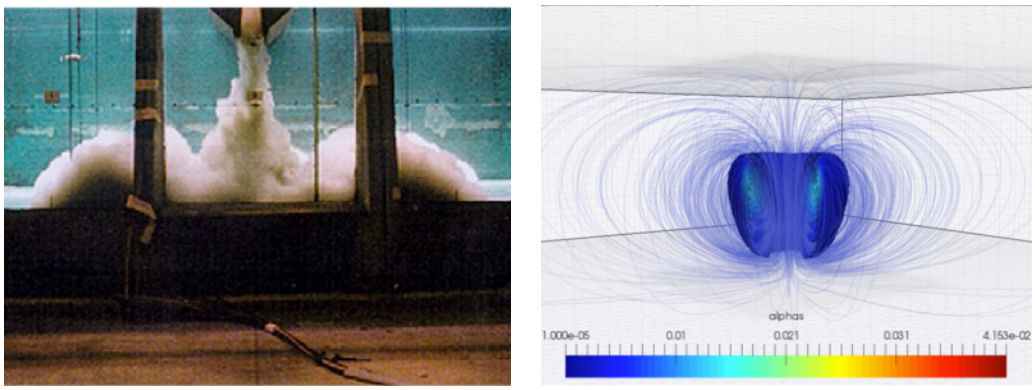

Figure 1. Experimental and preliminary two-phase flow numerical results of sediment release into homogenous water.

A numerical study on wave-driven ripple migration and benthic flux

Jiaye Zhang[1], Ali Salimi Tarazouj[1], Antoine Mathieu[1,3], Tian-Jian Hsu[1], Holly Michael[2]
[1]Civil and Environmental Engineering, University of Delaware, Newark, DE, USA
[2] Departments of Earth Sciences, University of Delaware, Newark, DE, USA
[3]LEGI, University of Grenoble Alpes, G-INP, CNRS, 38000 Grenoble, France

Two-dimensional turbulence-averaged simulations of bottom-slope-induced sediment transport via wave orbital ripples was conducted by utilizing the Eulerian two-phase flow model, SedFoam. Model results are analyzed to investigate benthic flux due to migrating ripples. The model is validated with the laboratory experiment of orbital ripples driven by sinusoidal oscillatory flow for three different slopes reported by Wang and Yuan (2018). Model results showed that the ripple equilibrium geometry becomes slightly upslope leaning with the increase of the bottom slopes ($\beta = 0^{\circ}$~2.6°). The simulated net sediment transport rates over the ripples are directed to the downslope (offshore) direction and increase linearly with the bottom slope. In comparison with the suspended load transport, the analysis indicated that the near-bed load transport is dominated during the entire wave period and contributes more to the increase of the net downslope sediment transport rates. Since the ripple migration is correlated with the near-bed sediment transport, the model results showed that the downslope ripple migration rates exhibit a good linear dependency on the bottom slopes (Figure 1a). The presence of ripple causes flow separation on either side of the ripple (Figure 1b) during the onshore and offshore phase. In the wave-averaged field, the flow separation causes a higher dynamic pressure near the ripple through and a lower dynamic pressure zone at the ripple crest (Figure 1c). The dynamic pressure gradient at the ripple surface leads to a notable circulation pattern in the permeable ripple bed; a flux from the boundary layer into the ripple at the trough and a flux from the sediment bed toward the ripple crest. It is worth noting that even though the ripple migration rates are different due to the bottom-slope effect, the dynamic pressure fields over the ripples are similar for these cases and hence the ripple migration rate is uncorrelated with benthic flux. In the conference, we will present more analyses on ripple migration and benthic flux driven by skewed and asymmetric oscillatory flows and preliminary simulations using 3D Large-eddy simulation.

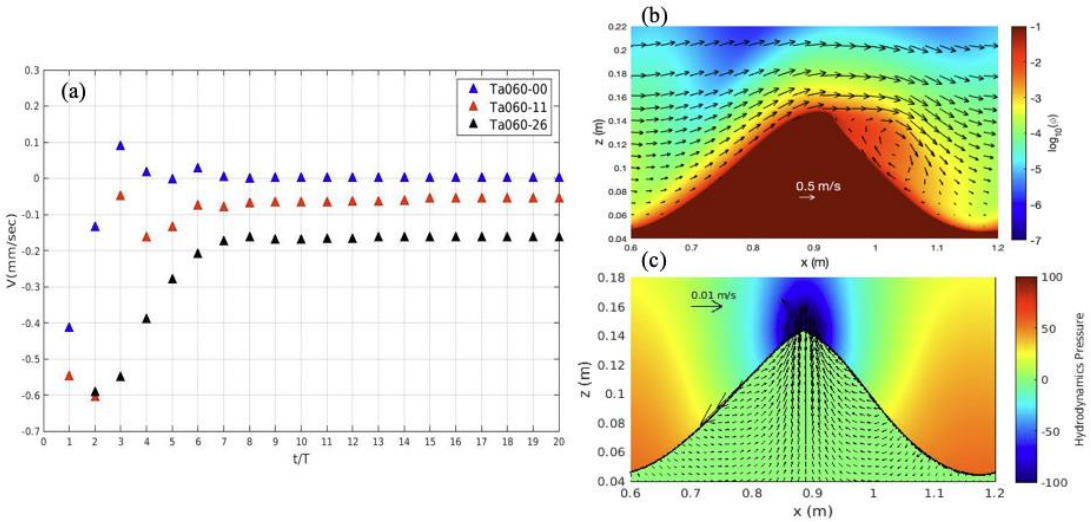

Figure 1: (a) Comparison of ripple migration rates for three different bottom slopes. (b) Sediment concentration field and down-sampled fluid velocity for Case TA060-26 (bottom-slope of 2.6°) at the instant of onshore flow deceleration. (c) Wave-period-averaged dynamic pressure field for Case TA060-26 and the resulting wave-period-averaged water volume flux in the ripple.

Reference

Wang, D., & Yuan, J. (2018). Bottom-Slope-Induced Net Sediment Transport Rate Under Oscillatory Flows in the Rippled-Bed Regime. Journal of Geophysical Research: Oceans, 123(10), 7308-7331.

A numerical study on wave-driven ripple migration and benthic flux

Jiaye Zhang[1], Ali Salimi Tarazouj[1], Antoine Mathieu[1,3], Tian-Jian Hsu[1], Holly Michael[2]
[1]Civil and Environmental Engineering, University of Delaware, Newark, DE, USA
[2] Departments of Earth Sciences, University of Delaware, Newark, DE, USA
[3]LEGI, University of Grenoble Alpes, G-INP, CNRS, 38000 Grenoble, France

Two-dimensional turbulence-averaged simulations of bottom-slope-induced sediment transport via wave orbital ripples was conducted by utilizing the Eulerian two-phase flow model, SedFoam. Model results are analyzed to investigate benthic flux due to migrating ripples. The model is validated with the laboratory experiment of orbital ripples driven by sinusoidal oscillatory flow for three different slopes reported by Wang and Yuan (2018). Model results showed that the ripple equilibrium geometry becomes slightly upslope leaning with the increase of the bottom slopes ($\beta = 0^{\circ}$~2.6°). The simulated net sediment transport rates over the ripples are directed to the downslope (offshore) direction and increase linearly with the bottom slope. In comparison with the suspended load transport, the analysis indicated that the near-bed load transport is dominated during the entire wave period and contributes more to the increase of the net downslope sediment transport rates. Since the ripple migration is correlated with the near-bed sediment transport, the model results showed that the downslope ripple migration rates exhibit a good linear dependency on the bottom slopes (Figure 1a). The presence of ripple causes flow separation on either side of the ripple (Figure 1b) during the onshore and offshore phase. In the wave-averaged field, the flow separation causes a higher dynamic pressure near the ripple through and a lower dynamic pressure zone at the ripple crest (Figure 1c). The dynamic pressure gradient at the ripple surface leads to a notable circulation pattern in the permeable ripple bed; a flux from the boundary layer into the ripple at the trough and a flux from the sediment bed toward the ripple crest. It is worth noting that even though the ripple migration rates are different due to the bottom-slope effect, the dynamic pressure fields over the ripples are similar for these cases and hence the ripple migration rate is uncorrelated with benthic flux. In the conference, we will present more analyses on ripple migration and benthic flux driven by skewed and asymmetric oscillatory flows and preliminary simulations using 3D Large-eddy simulation.

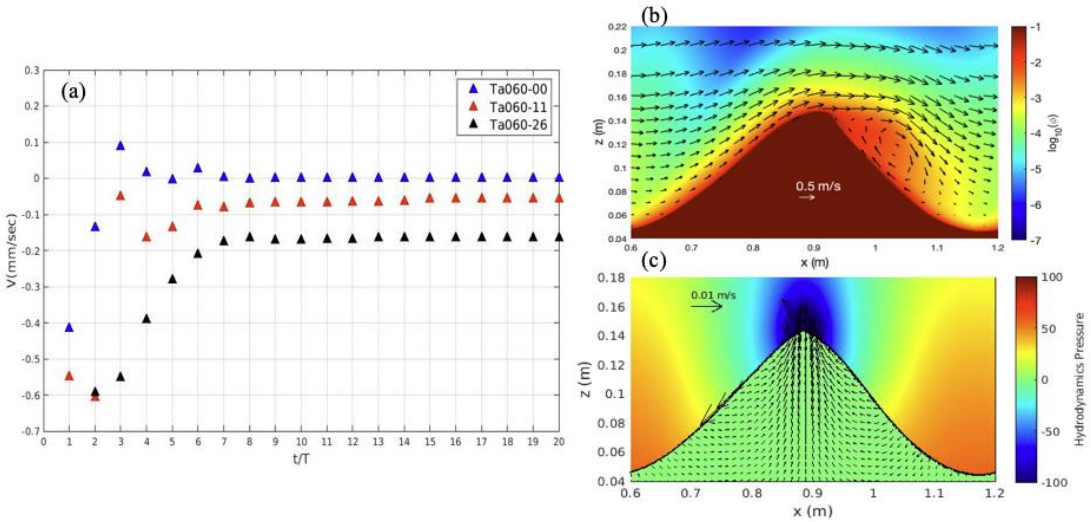

Figure 1: (a) Comparison of ripple migration rates for three different bottom slopes. (b) Sediment concentration field and down-sampled fluid velocity for Case TA060-26 (bottom-slope of 2.6°) at the instant of onshore flow deceleration. (c) Wave-period-averaged dynamic pressure field for Case TA060-26 and the resulting wave-period-averaged water volume flux in the ripple.

Reference

Wang, D., & Yuan, J. (2018). Bottom-Slope-Induced Net Sediment Transport Rate Under Oscillatory Flows in the Rippled-Bed Regime. Journal of Geophysical Research: Oceans, 123(10), 7308-7331.

Two-phase modelling of sediment transport by incompressible SPH

Yan Zhou[1,2] and Ping Dong[1]

[1] School of Engineering, University of Liverpool, UK
[2] State Key Laboratory of Hydrology-Water Resources and Hydraulic Engineering, Hohai University, China

Sediment transport has been broadly modelled from the conventional convection-diffusion equation to sophisticated individual grain tracking method with various demands of empirical coefficients and computational resources. This study develops a new two-phase Lagrangian model under the framework of incompressible smoothed particle hydrodynamics (ISPH) for sediment movement which is fully coupled with the flow through inter- and intra-phase interactions. By adopting single set of particles representing parcels containing both fluid and sediment, concentration, velocity for each phase and fluid pressure will be obtained by solving Navier-Stokes equation for each phase. The incompressible scheme enables stable fluid pressure simulation by implicitly solving fluid pressure Poisson equation. The model will be validated by static neutral buoyant case for testing the stability, sediment settling against analytical solution and sand dumping for testing complex flow and sediment concentration fields development.

Grain-resolving simulations of submerged cohesive granular collapse

Rui Zhu[1;2], Zhiguo He[1], Kunpeng Zhao[3], Bernhard Vowinckel[4], and Eckart Meiburg[2]

[1]Ocean College, Zhejiang University, Zhoushan, 316021, China

[2]Department of Mechanical Engineering, UC Santa Barbara, Santa Barbara, CA 93106, USA

[3]State Key Laboratory of Multiphase Flow in Power Engineering, Xi'an Jiaotong University, Xi'an 710049, China

[4]Leichtweiss-Institut fuer Wasserbau, Technische Universitaet Braunschweig, 38106 Braunschweig, Germany

Abstract

We investigate the submerged collapse of weakly polydisperse, loosely packed cohesive granular columns, as a function of aspect ratio and cohesive force strength, via grain-resolving direct numerical simulations. The cohesive forces act to prevent the detachment of individual particles from the main body of the collapsing column, reduce its front velocity, and yield a shorter and thicker final deposit. All of these effects can be accurately captured across a broad range of parameters by piecewise power-law relationships. The cohesive forces significantly reduce the amount of available potential energy released by the particles. For shallow columns, the particle and fluid kinetic energy decreases for stronger cohesion. For tall columns, on the other hand, moderate cohesive forces increase the maximum particle kinetic energy, since they accelerate the initial freefall of the upper column section. Only for larger cohesive forces do the peak kinetic energy of the particles decrease. Computational particle tracking indicates that the cohesive forces reduce the mixing of particles within the collapsing column, and it identifies the regions of origin of those particles that travel the farthest. The simulations demonstrate that cohesion promotes aggregation and the formation of aggregates. They furthermore provide complete information on the temporally and spatially evolving network of cohesive and direct contact force bonds. While the normal contact forces are primarily aligned in the vertical direction, the cohesive bonds adjust their preferred spatial orientation throughout the collapse. They result in a net macroscopic stress that counteracts deformation and slows the spreading of the advancing particle front.

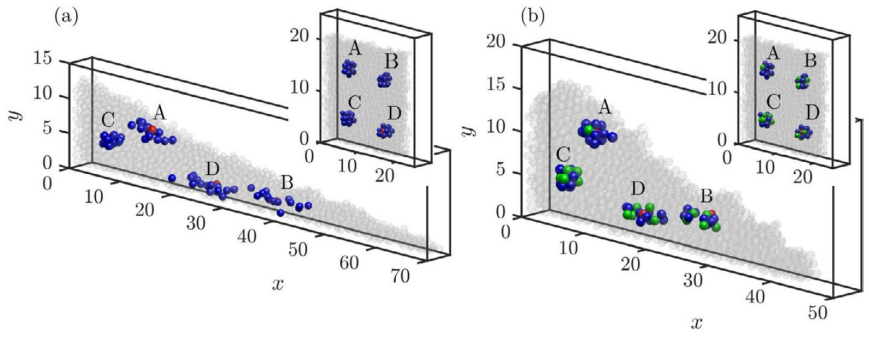

A study on vertical sorting mechanism in gravel bed rivers with graded sediment using the APM method

Takatoshi ATSUMI[1*], Shoji FUKUOKA[2]

[1] JSPS Research Fellow・Civil, Human and Environmental Engineering, Chuo University, 1-13-27 Kasuga, Bunkyo-ku, Tokyo 112-8551, Japan.
Tel.: +81 3 3817-1615, Email address: a14.c3y6@g.chuo-u.ac.jp

[2] Research and Development Initiative, Chuo University. E-mail address: sfuku@tamacc.chuo-u.ac.jp

* Corresponding author

Key Words: *gravel-bed rivers, sediment transport, vertical sorting, resolved CFD-DEM*

1. Introduction

Studies on armoring of grain size materials in gravel bed rivers have been investigated actively. Many models have been attempted to evaluate sorting mechanism of bed materials on grain size profiles and shielding effects. There are still issues to be addressed in the modeling of bed variation analysis method with assumptions for simplifications (e.g., neglecting interactions between moving particles and assuming no movement of large particles in the riverbed). In bed variation analysis models, the bed load is often evaluated based on the processes of entrainment, transport, and deposition. In particular, it is important to properly evaluate the entrainment and deposition rate, which are directly related to changes in the riverbed structure.

Physical Experimental observations have limitations in obtaining detailed mechanism of each particle motion in graded sediment. On the other hand, numerical approaches have advantages for analyzing space and time variation motions on each particle motion. Fukuoka et al.[1)] developed APM method (a type of resolved-CFD-DEM model) that can directly analyze solid-liquid phase interactions, and obtain trajectories, velocities, and distributions of gravel particles flowing on a fixed bed. They compared the computational result with experimental results and showed the validation of their APM model.

In this study, APM method applied for gravel bed with a wide distribution of grain-size of one order of magnitude in order for better understanding the mechanism of the bed load. And the vertical sorting mechanism of the bed structure was analyzed and discussed on the basis of the data of particles movement for each grain size obtained by this numerical computation.

2. Numerical methods

The numerical simulation model of Fukuoka et al. [1)] is used for this investigation. Fluid motions were simulated using the governing equations of a single-fluid model for the solid-liquid multiphase flows in the Eulerian approach. Particle motions were computed by the Lagrangian approach using DEM method. The free-surface variation was simulated using the continuity equation of the fluid volume fraction based on the volume-of-fluid (VOF) method. The particle motion was simulated using the momentum and angular momentum equations as a rigid body. The parameters used in the simulation re shown in Table 1.

Table. 1 Simulation parameters.

cell size	0.00375	m
Time step for the fluid simulation	5×10^{-5}	s
Time step for the particle simulation	2.0×10^{-6}	s
Density of water	1,000	kg/m^3
Density of particles	2,650	kg/m^3
Fluid viscosity	8.9×10^{-4}	Pa・s
Smagorinsky constant	0.173	-
Elastic modulus	5×10^{10}	Pa
Poisson's ratio	0.33	-
restitution coefficient	0.7	-
Friction Coefficients	0.5	-

Table. 2 Experimental conditions.

Water discharge Q	3.99	m^3/s
Water depth	0.93	m
Froude number	1.39	-
mean bed elevation	0.26	m
Packing depth	0.31	m
bed slope	1/30	-

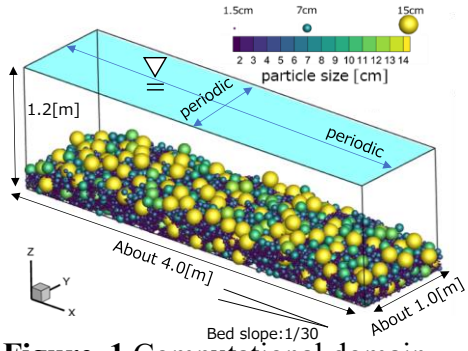

Figure. 1 Computational domain and boundary conditions.

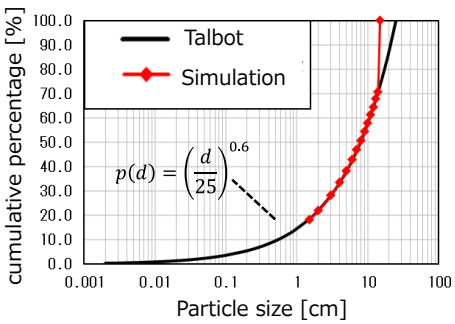

Figure. 2 Particle size distribution.

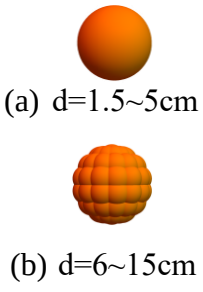

Figure. 3 Particle shape.

3. Experimental conditions

Figure 1 shows the Computational domain, coordinate axes and boundary conditions. The numerical channel is 4.01 m long, 1.01 m wide with a bed slope of 1:30. The periodic boundary condition was applied to the longitudinal and transverse boundaries. Figure 2 shows the particle size distribution used in the numerical experiment. The particle size distribution is set based on the Talbot type and has a spread of one order, d=1.5~15 cm. Figure 3 shows the particle shapes used in the numerical analysis. In order to speed up the calculation, a single sphere shape was used for particle sizes d=1.5~5 cm, as shown in Figure-3(a), and for particle sizes d=6~15 cm, several small spheres without gap were connected to form a spherical shape, as shown in Figure-3(b).

The particles were packed randomly to make a riverbed. The Initial water level was set to 1.2m. Table 2 shows the experimental conditions. The mean bed elevation was calculated by the bed particles with velocity less than 0.05 m/s. The water depth and the Froude number were calculated by spatially averaged over the entire simulation area.

4. Simulation Results

Figure 4 shows gravel bed structures on the vertical plane at t=0 and 50s. From the comparison of Figures. 4 (a) and 4 (b), it can be seen that vertical sorting of particles occurs in the surface layer of the riverbed and the particles below z=0.15 m does not shift at all. Figure-5 shows the temporal variation of the vertical distribution of the solid volume concentration, spatially averaged over the entire analysis area in the x-y plane. Figures 5 (b), (c) and (d) show the solid volume fractions of large, medium and small particles, respectively. In Figure 5(b), the volume fraction around z = 0.20 m is particularly reduced. This is due to the vertical upward displacement of large particles, which were initially buried in the surface layer. On the other hand, the small particles shown in Figure 5(d) drop into the pore spaces between the large and medium particles and are displaced vertically downward. As a result, the volume fraction of the layer above z=0.20m decreases, and the volume fraction below

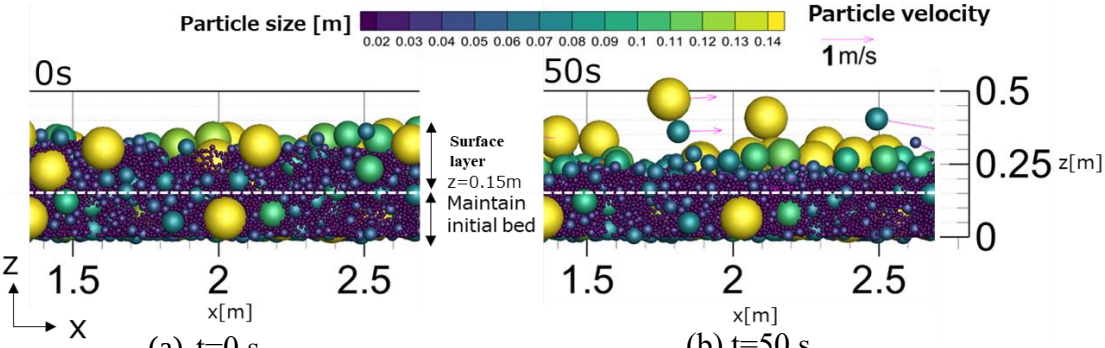

(a) t=0 s (b) t=50 s

Figure. 4 Time change of riverbed structure.

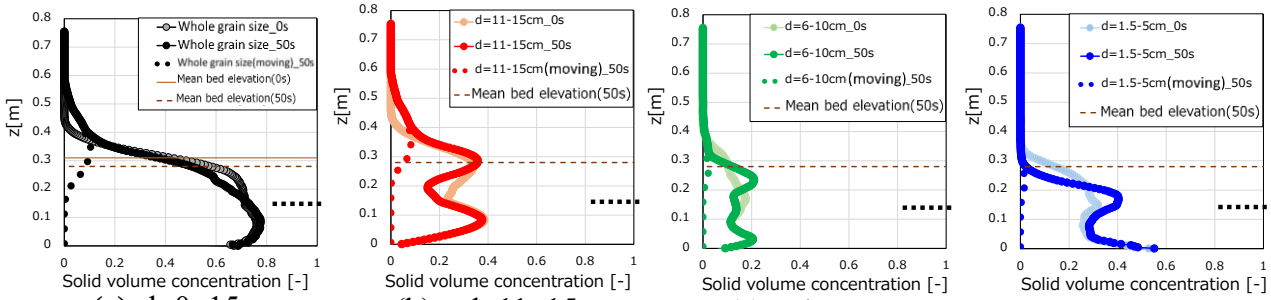

(a) d=0~15cm (b) d=11~15cm (c) d=6~10cm (d) d=1.5~5cm

Figure. 5 Vertical distribution of solid volume concentration.

z=0.20m increases. In Figure 5(c), the volume fraction of medium particles at z = 0.10~0.20m and above z = 0.30m decreased due to both the rise of buried particles and the drop of exposed particles.

Next, the entrainment and deposition rate, which are related to the armoring of the mixed particles are calculated. Now consider an arbitrary control volume (C.V.), and the continuity equation for the solid phase is ,

$$\frac{\partial V_s^k(x,y,z,t)}{\partial t} = Q_{in}^k(x,y,z,t) - Q_{out}^k(x,y,z,t) \tag{1}$$

where V_s:volume of solid phase [m^3],Q_{in}: volume of solid phase flowing into C.V. per unit time [m^3/s] and Q_{out}: volume of solid phase flowing out of C.V. per unit time [m^3/s]. k indicates particle numbers.

If we divide the volume of the solid phase V_s into the volume of moving particles V_{sm} and the volume of bed (stationary) particles V_{sb}, and consider the continuity equation, we can write the following for V_{sm} and V_{sb} respectively.

$$\frac{\partial V_{sm}^k(x,y,z,t)}{\partial t} = E^k(x,y,z,t) - D^k(x,y,z,t) + Q_{in}^k(x,y,z,t) - Q_{out}^k(x,y,z,t) \tag{2}$$

$$\frac{\partial V_{sb}^k(x,y,z,t)}{\partial t} = D^k(x,y,z,t) - E^k(x,y,z,t) \tag{3}$$

$$V_s^k(x,y,z,t) = V_{sm}^k(x,y,z,t) + V_{sb}^k(x,y,z,t) \tag{4}$$

where D: deposition rate [m3/s], E: entrainment rate [m3/s]. D and E are the volume of particles deposited from moving particle to bed particle and the volume of particle detached from bed particle to moving particle within the C.V. per unit time, respectively.

Figure.6(a)~(c) shows the vertical distributions of the entrainment and deposition rates for respective particle sizes (d=1.5,6-9,15 cm). The C.V. was set as follows: channel width (4.02 m) in the longitudinal direction, channel length (1.02 m) in the transverse direction, and 5 cm each in the vertical direction. And the C.V. to which each particle belongs is determined from the position of the particle center of gravity. The entrainment and deposition judgement are made for each particle every 10 s.

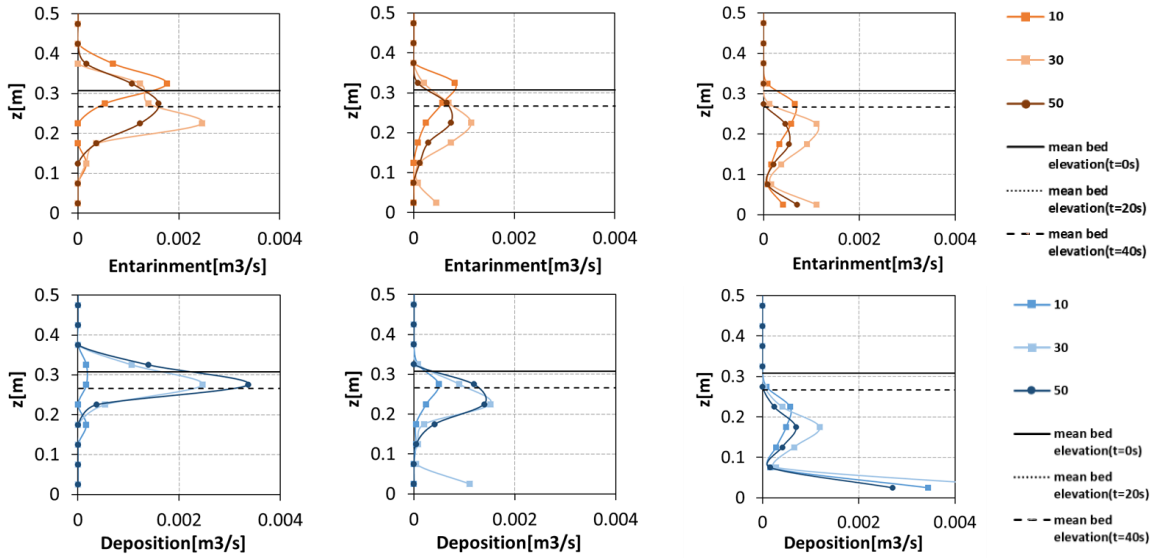

(a)d=15cm (b)d=6-9cm (c)d=1.5cm

Figure. 6 Vertical distributions of Entrainment and Deposition rate

Entrainment was evaluated when the particle velocity was greater than 5 cm or when the C.V. belonging to the particle at the time of judgement was different from the C.V. before 10 s. Deposition was evaluated when the particle velocity was less than 5 cm or when the C.V. belonging to the particle at the time of judgement was different from the C.V. before 10 s. The amount of entrainment (or deposition) is given by each particle volume for the C.V. to which it belonged before 10s.The volume of entrainment and deposition in each C.V. was divided by the observation time of 10 s to obtain E and D as values per unit time.

In terms of the vertical distribution of D, the larger the grain size is, the higher the vertical position of deposition occurs, and the temporal change in vertical distribution is relatively small for each particle size. In the vertical distribution of E, as in the vertical distribution of D, the larger the particle size is, the higher the particle detachment occurs. In particular, for all grain sizes, the Entrainment occurs at higher vertical positions at t=0-10s. Thus, for each particle size, as the water flow began, the surface particles were detached, and when moving particles were deposited, the large particle size group stayed at a higher position on the surface, and the small particle size group was deposited at a lower position, resulting in formation of vertical sorting.

In particular, at t=40-50s, the vertical distributions of E and D tend to be similar for each grain size. Therefore, from equation (3), the time variation of the vertical distribution of the volume of bed particles for each grain size becomes small, and the bed structure reaches an equilibrium state.

5. Conclusion

A numerical movable-bed experiment of the mixed particle size was conducted to investigate the vertical distribution of the entrainment and deposition rate, and to better understand the formation mechanism of vertical sorting.

6. Acknowledgment

This work was supported by JSPS KAKENHI Grant Number JP20J22413.

References

[1] Fukuoka, S., Fukuda, T., Uchida, T., 2014. Effects of sizes and shapes of gravel particles on sediment transports and bed variations in a numerical movable-bed channel, *Adv. in Water Res.*, 72, 84-96, https://doi.org/10.1016/j.advwatres.2014.05.013.

Movement mechanism of boulders composing valley bank and beds by debris flows and development of debris flow front using the APM method

Hiroki Kato[1*], Shoji Fukuoka[2]
[1]Civil, Human and Environmental Engineering, Chuo University, 1-13-27 Kasuga, Bunkyo-ku, Tokyo 112-8551, Japan
[2] Research and Development Initiative, Chuo University, 1-13-27 Kasuga, Bunkyo-ku, Tokyo 112-8551, Japan.
* Corresponding author. Tel.: +81 3 3817-1615. E-mail address: a17.jnt5@g.chuo-u.ac.jp.

keyword : *debris flow, valley bank and bed erosion, the one-fluid model of solid-liquid multiphase, APM method*

1. Introduction

Clarifying the erosion mechanism of a valley by a debris flow is important not only for evaluating the amount of debris flow that passes through the valley, but also for evaluating the stability of the valley beds and banks after the debris flow has passed. However, the erosion mechanism of valley beds and banks by debris flows has not been fully clarified.

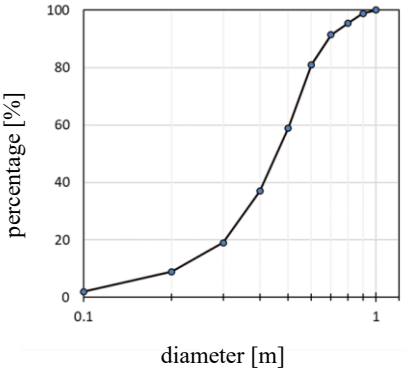

Fig. 1 Particle size distribution

Iverson et al. [1] measured the total stress and pore water pressure acting on the channel bed during debris flow passage using large scale model experiments, and showed that the momentum of the debris flow is increased by entrainment due to liquefaction of the channel bed. Lyu et al. [2] focused on bank erosion caused by the passage of debris flow and compared the flow and erosion between cases where bank erosion is dominant and cases where only bed erosion occurs. The results show that valley bank erosion contributes more to the growth of the debris flow front than bed erosion, and that valley bank erosion occurs after the front of debris flow has passed.

However, it is difficult to measure the forces acting on individual particles and the flow field around the particles in these model experiments, which can only be done by numerical analysis. Euler-Euler type approach is less computationally demanding than the Euler-Lagrange type approach and analyzes in the field scale. But it does not elucidate the essential phenomena of the debris flow. In recent years, with the improvement of computer performance, the Euler-Lagrange type model has been developed. Fukuda et al. [3] developed the Euler-Lagrange type model (APM method) that can analyze non-spherical particles, and explained the results of the debris flow channel experiment conducted by Ito et al.

In this study, as basic research on the erosion mechanism of valley bank and bed, a straight valley shape with mobile valley bed and bank is created. The results of the numerical experiment are compared with the results of the model experiment and the factors causing the movement of individual particles are discussed.

2. Numerical methods

2.1. Numerical method of fluid motions

In the flow analysis with the stone and gravel particles, a one-fluid model of solid-liquid multiphase flow is used, where the solid phase is given as a fluid with different densities, and the whole is assumed to be an incompressible fluid. The basic equation of the flow is shown below.

$$\frac{\partial u_i}{\partial x_i} = 0 \tag{1}$$

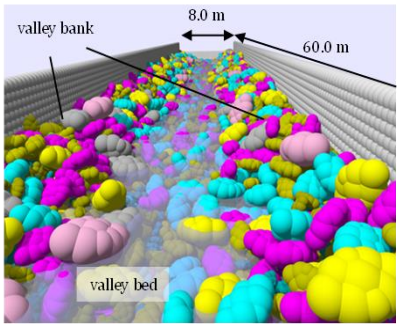

Fig. 2 Initial state

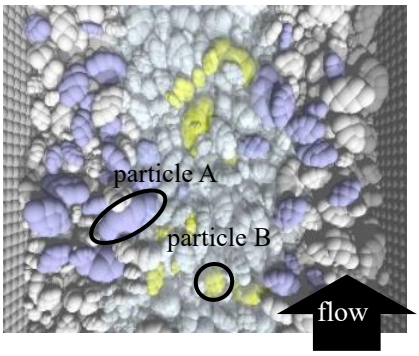

Fig. 3 State of before the passage of the debris flow front

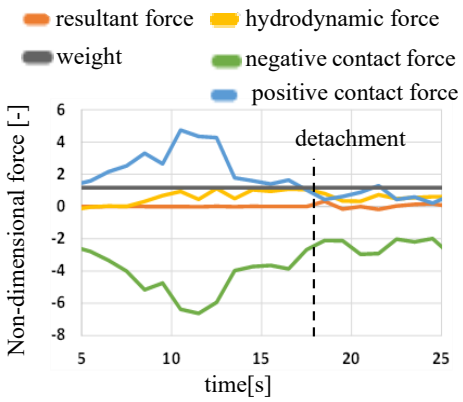

(a) Particle A

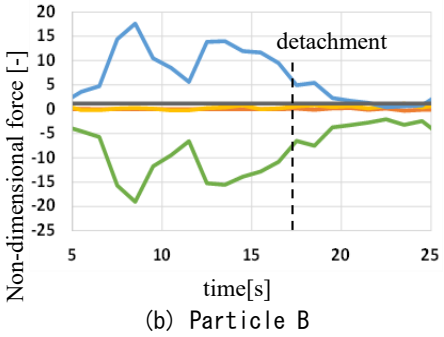

(b) Particle B

Fig. 4 Time variation of the longitudinal non-dimensional force

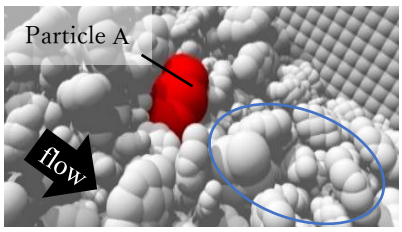

(a) Just before the arrival of the debris flow front

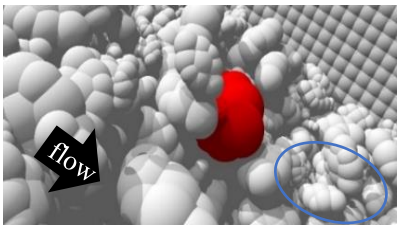

(b) Just before particle A starts to move

Fig. 5 stone and gravel around particle A

$$\frac{\partial u_i}{\partial t} + u_j \frac{\partial u_i}{\partial x_j} = g_i - \frac{1}{\rho}\frac{\partial P}{\partial x_i} + \frac{\partial}{\partial x_j}\{2(\nu + \nu_t)S_{ij}\} \tag{2}$$

$$\nu_t = (C_s\Delta)^2\sqrt{2S_{ij}S_{ij}} \tag{3}$$

where ρ and u_i are the volume average density and the mass average velocity, respectively, taking into account the volume fraction of the particles in a computation grid. ν is the kinematic viscosity, g_i is the gravitational acceleration, P is the sum of the isotropic components of pressure and SGS stress, S_{ij} is the strain rate tensor, ν_t is the turbulent viscosity, and C_s is the Smagolinsky constant. Δ is the computation grid size. The free water surface was simulated using the volume of fluid (VOF) method.

2.2. Numerical method of gravel motions

The motion of the particles is solved using the equation of motion of a rigid body, and the contact judgment and contact force of the gravels are evaluated using the distinct element method for each gravel particle. The hydrodynamic forces on the particles are calculated directly by volume integration of the pressure and diffusion terms in the equation of motion of the flow field. The basic equations are shown below.

$$M\ddot{r}_i = Mg_i + F_i^f + F_i^c \tag{4}$$

$$\dot{\omega}_{i'} = I_{i'j'}^{-1}\{R_{j'i}(T_i^f + T_i^c) - \varepsilon_{j'k'l'}\omega_{k'}I_{l'm'}\omega_{m'}\} \tag{5}$$

where, where the index i denotes the components of the global coordinate system fixed on the space, the indices i'–m' denote the components of the local coordinate system fixed on a rigid body, M is the mass of a particle, r_i^g is the position of the center of gravity of the rigid body, ω_i is the angular velocity, F_i is the force acting on the surface of the particle, and T_i is the torque on the center of the gravity generated by the force. The superscripts f and c are the components of the fluid forces and contact forces between particles, respectively, g_i is the gravitational acceleration, $I_{i'j'}^{-1}$ is the inverse of the matrix consisting of the components of the moment of inertia tensor in the local coordinate system, $R_{j'i}$ is equal to $\boldsymbol{e}_{j'} \cdot \boldsymbol{e}_i$ ($\boldsymbol{e}_{j'}$ and $\boldsymbol{e}_i$ are unit basis vectors), and $\varepsilon_{j'k'l'}$ is the Levi–Civita symbol.

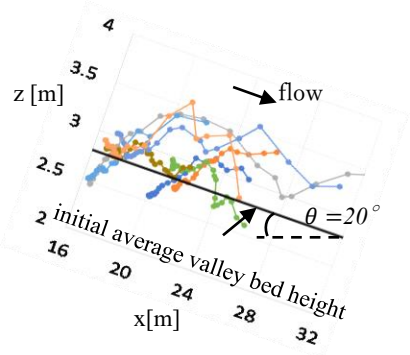

(a) Particle with a diameter of more than 0.5m

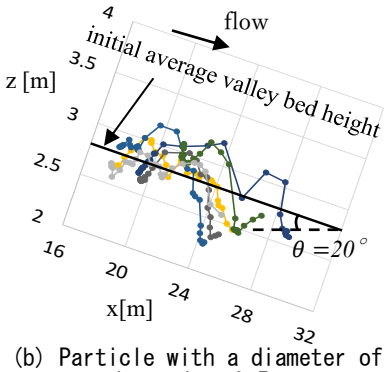

(b) Particle with a diameter of less than 0.5m

Fig.6 Position of the center of gravity for each of the particles

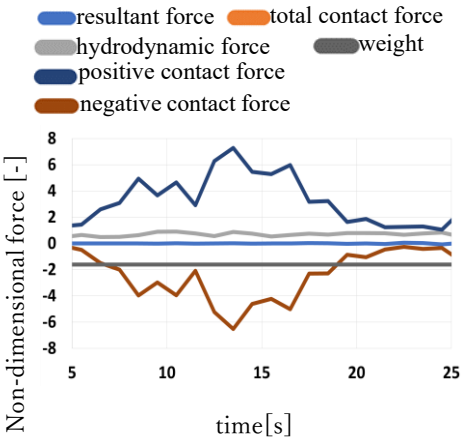

Fig.7 Time variation of the non-dimensional vertical force acting on particle B

3. Experimental conditions of the numerical movable-bed channel

The numerical movable-bed channel used in this study is a straight channel of 60 m in length and 8 m in width. The slope of the channel was set to 20°. The coordinate axes are the x-axis in the downstream direction, the y-axis in the transverse direction, and the z-axis in the upward direction (the z-axis direction is referred to as the vertical direction). We used non-spherical particles of the valley bed and bank consisting of 10 different particle sizes, with the largest particle size being 1.0 m and the smallest being 0.1 m, as shown in Figure 1. All the particles are equal in shape and density. The diameters of non-spherical particles were defined as the diameters of spheres with the same volume.The particles were randomly dropped into the channel, and the initial channel form was set up with the slope of the valley bank at about 30 degrees and is shown in Figure 2. In the experiment, a constant flow rate of 10.0 $[m^3/s]$ was continuously applied at the upstream end of the channel. No sediment was supplied to the flowing water. At the downstream end, the pressure was set to zero and the sediment was discharged out freely. The debris flow front was formed by taking particles from the valley bed and bank.

4. Movement mechanism of valley bank and bed particles

We focused on particles that had moved more than 5 meters in the longitudinal direction from the section where the debris flow front had passed. In Figure 3, the blue particles are the valley bank particles and the yellow particles are the valley bed particles. The number of valley bank particles and bed particles we focused on was 38 and 14, respectively.

4.1. Movement mechanism, of valley bank particles

The main force causing the movement of 38 sample particles of the valley bank was as follows: 1 particle was due to hydrodynamic forces, 5 due to collision forces, 23 due to a decrease in resistance force, and 9 due to other factors. The decrease in the resistance force implies the decrease in the contact force and brought the start of the longitudinal movement of the valley bank particles. Figure 4 demonstrates time variations of the longitudinal force acting on particles A and B shown in Figure 3. The positive contact force and fluid force on particle A in Figure 4(a) increase with the arrival of the debris flow front. However, the negative contact force also increases, and the resultant force becomes zero and the particle does not start to move. At about 18 seconds after the arrival of the debris flow front, particle A starts to move, although the force is smaller than when the debris flow front arrived. Figure 5 shows the state of the gravel around particle A just before the arrival of the debris flow front and just before the start of movement. The red particle is particle A. Figure 5 shows that just before the arrival of the debris flow front, the particles on the downstream side of the debris flow are firmly interlocked, taking placement where they can produce a large resistance force. On the other hand, just before particle A starts to move, the surrounding stones and gravels break down their alignment. Particularly, the particles on the downstream side have been shifted, and particle interlocking has taken worse alignment. It is thought that the resistance force of the site is smaller than that before the arrival of the debris flow front, and this causes the valley bank particles to start moving and the scale of debris flow front to grow.

4.2. Movement mechanism, of valley bed particles

The movement of particles that make up the valley bed were analyzed in the same way as that of the particles that form the valley bank. The 14 specimens were examined. The main factor that caused the particles to start moving in the longitudinal direction was hydrodynamic force (2 specimens), collision (1 specimen), reduced resistance (11 specimens), and other factors (0 specimens). The main factor in the movement of the particles that make up the valley bed is a decrease in the resistance force. Figure 4(b) shows that, when the debris flow front reaches particle B, both the hydrodynamic force and the positive contact force increase, and the negative contact force also increases, like particle A, so the resultant force is zero and the particle does not start moving. After that, the particle started to move with less force than when the debris flow front arrived.

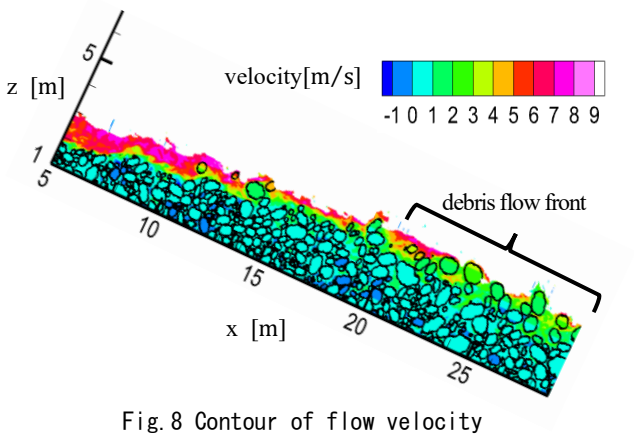

Fig. 8 Contour of flow velocity

Figure 6 shows change in the position of the center of gravity for each of the particles of interest in the valley bed. Figure 6 shows that the particles on the surface of the valley bed first move vertically upward, and then begin to move longitudinally. It is thought that the particles of the valley bed begin to move because they decrease contact force in the negative direction by moving vertically upward. In addition, for particles in the valley bed, the smaller particles moved to a lower position in relation to the initial valley bed. It is thought that the smaller particles drop among the larger particles.

The particles on the valley bed surface began to move at about 18.6 seconds. This is the time when the rearmost part of the debris flow front is passing through the location of the particles of interest. In other words, the particles on the surface of the valley bed begin to move not when the debris flow front arrives and exerts a large force, but when the debris flow front passes by.

Figure 7 shows the time variation of the non-dimensional vertical force acting on particle B. The absolute value of the contact force in the negative direction increases with the arrival of the debris flow front. It is thought that the force is exerted to the vertical downward direction from the particles constituting the debris flow front, which acts as a resistance force and prevents the particles from starting to move.

Figure 8 shows the velocity contour map during the passage of the debris flow front. It is seen that the velocity of the debris flow front is small, while the velocity of the following flow is large. This is similar to the experimental results of Lyu et al. [2]. Unstable gravel and stone particles on the bed of the channel after the debris flow front passed through are supplied into the front of debris flow by the fast flow of the following stream.

5. Conclusion

In this study, the erosion mechanisms of individual particles in a valley were investigated using the APM method. The results of numerical experiments were similar to those of previous experimental studies. The particles on the bank and bed of the valley are eroded due to a decrease in resistance force. Valley bank particles had reduced resistance due to the discharge of downstream particles, and valley bed particles had reduced resistance due to moving to a relatively higher position than the surrounding particles. It is clear that particles initiating migration by such a mechanism is transported to the debris flow front by the following flow and that a debris flow develops.

References

[1] Richard M. Iverson, Mark E. Reid, Matthew Logan, Richard G. LaHusen, Jonathan W. Godt and Julia P. Griswold: Positive feedback and momentum growth during debris-flow entrainment of wet bed sediment, Nature Geoscience, Volume 4, pp.116-121, 2011

[2] Richard M. Iverson, Mark E. Reid, Matthew Logan, Richard G. LaHusen, Jonathan W. Godt and Julia P. Griswold: Positive feedback and momentum growth during debris-flow entrainment of wet bed sediment, Nature Geoscience, Volume 4, pp.116-121, 2011

[3] Fukuoka, S., Fukuda, T., Uchida, T., 2014. Effects of sizes and shapes of gravel particles on sediment transports and bed variations in a numerical movable-bed channel, *Adv. in Water Res.*, 72, 84-96, https://doi.org/10.1016/j.advwatres.2014.05.013.

Effects of particle volume and shape on saltation motion of single particle in a turbulent flow over roughened bed

Yuya Takakuwa[1*], Shoji Fukuoka[1]

[1] Research and Development Initiative, Chuo University, 1-13-27 Kasuga, Bunkyo-ku, Tokyo 112-8551, Japan.

*Corresponding author. Tel.: +81 3 3817-1617. E-mail address: ytakakuwa099@g.chuo-u.ac.jp

Key Words: *Non-spherical particle, Movement manner, Instantaneous particle velocity, Fluid forces and collision forces, the APM method*

1. Introduction

Motions of particles in a turbulent flow over a roughened bed are controlled by hydraulic conditions, particle properties (physical properties, volume, and shape), bed roughness, particle-particle interactions, and fluid-particle interactions. We have assumed in previous sediment transport studies that the particle shape is spherical. However, effects of the particle shape cannot be neglected when dealing with large size particles, such as in bed variations in gravel-bed rivers. Effects of the particle shape on saltation motions have been investigated by focusing on the time-averaged particle velocity and hop length and height [1],[2], and there are few investigations about instantaneous particle velocity and forces acting on a moving particle. The Arbitrary Particle Multiphase method (the APM method [3]), a kind of Resolved CFD-DEM, is an effective method to solve these problems. Takakuwa and Fukuoka [4] performed the APM numerical simulations on saltation motion experiments [5] of single natural gravel with different volumes and shapes, and showed that the APM method can explain the transport process and the instantaneous velocity of non-spherical particles.

In this paper, effects of volume and shape on moving particle are clarified from time-averaged and instantaneous particle velocity, and fluid and collision forces of saltation motions of 12 particles with different volumes and shapes.

2. Computational setup and numerical scheme

As shown in Fig.1, a steady flow discharge 0.5 m^3/s is supplied from the upstream end (x = 0.0 m) of a straight channel with 45 m length, 1.08 m width and 1/20 bed slope, and a single particle is gently dropped from a height of 40 cm at x = 2.5 m, which follows the Shigemura's experiment [5]. The cross-sectional shape of the channel is designed to be a parabola, where particles tend to concentrate in the center of the channel. The channel bed was uneven due to the abrasion because the main aim of the Shigemura's experiment was understanding of abrasion mechanism of the channel bed by moving particles. The roughness at the bed is set by trial and error by superposing small spheres to reproduce the depth $\tilde{\bar{h}}^{Exp.}$ and the water surface velocity $\tilde{\tilde{u}}_s^{Exp.}$ measured by the Shigemura's experiment. The velocity distribution at x = 1.5 m is given at the upstream end in every time step to make the boundary

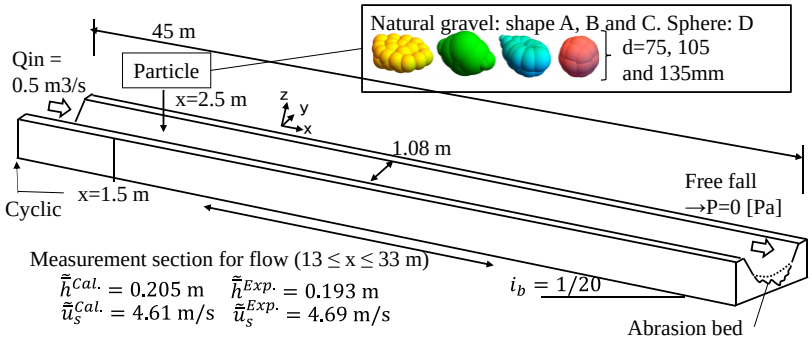

Figure. 1 Overview of numerical simulations.

Table. 1 Particle shapes. "a, b, and c" denote the longest, intermediate, and shortest axes, respectively. Dimensionless maximum projected area PA*max is the maximum projected area of the particle divided by that of the sphere with equivalent volume.

Shape name	a/d	b/d	c/d	Shape Factor = c/(ab)^0.5	Zingg's shape type	PA^*_{max}
A [6]	1.50	1.00	0.60	0.49	Disk	1.61
B [6]	1.39	1.01	0.79	0.67	Massive and symmetric	1.21
C [6]	1.34	0.90	0.83	0.76	Massive and asymmetric	1.25
D: Sphere	1.01	0.99	0.99	0.99	Massive	1.02

layer develop in the short distance. At the downstream end, a zero pressure is given for the free-fall flow in the experiment. 12 particles are used, consisting of 3 sizes (d = 75, 105, and 135 mm) and 4 shapes (see Fig.1 and Tab. 1. Natural gravel [5]: A Disk type, B Massive and symmetric type, C Massive and asymmetric type. D Sphere type). In this study, the particles are named by denoting their shapes and sizes, such as "A105".

The APM method [3] is a one of a Euler-Lagrange solvers. The fluid forces acting on an arbitrary shaped particle are directly calculated by detailed flows evaluated using a computational grid that is sufficiently smaller than a particle. Point collisions and areal contacts between particles and channel boundaries are evaluated by applying the Distinct Element Method (the Voigt model) to each small sphere making up a particle and a channel bed. Physical and numerical parameters are shown in Tab. 2.

Tab. 3 shows flow and channel characteristics. Fig.2 demonstrates time-averaged flow structures at x = 22.5 m. A high velocity of about 3.7 m/s is calculated at the channel center (y = 0.0 m), 0.05 m above the bottom, and secondary flows of Prandtl's second kind are also calculated in the corner between the bottom and the sidewall.

Table. 2 Physical and numerical parameters.

Density of fluid	1000	kg/m3
Density of particle	2500	kg/m3
Fluid viscosity	0.0010	kg/(m s)
Elastic modules	5.0E+10	Pa
Poisson's ratio	0.23	-
Coefficient of restitution	0.30	-
Coefficient of friction	0.20	-
Grid size	0.008	m
Number of grids (Nx*Ny*Nz)	5.7E+07 (=5629*147*69)	-
Time step for fluid calculation	2.0E-04	s
Time step for paritcle calculation	2.0E-06	s

Table. 3 Flow and channel characteristics at the channel center (y = 0.0 m).

Equivalent roughness	0.023	m
Depth	0.205	m
Depth-averaged velocity	3.88	m/s
Friction velocity	0.32	m/s
Froude number	2.73	-
Bulk Reynolds number	7.96E+05	-
Friction Reynolds number	6.53E+04	-
Shields number (d = 0.075, 0.105, 0.135)	0.092, 0.066, 0.051	-
d/ks (d = 0.075, 0.105, 0.135)	3.26, 4.57, 5.87	-

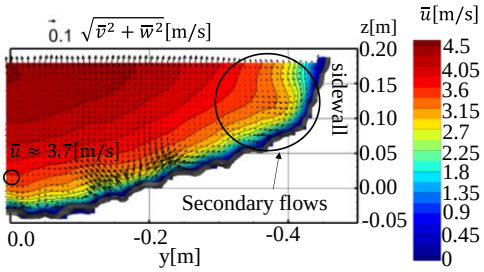

Figure. 2 Time-averaged flow structures at x = 22.5 m.

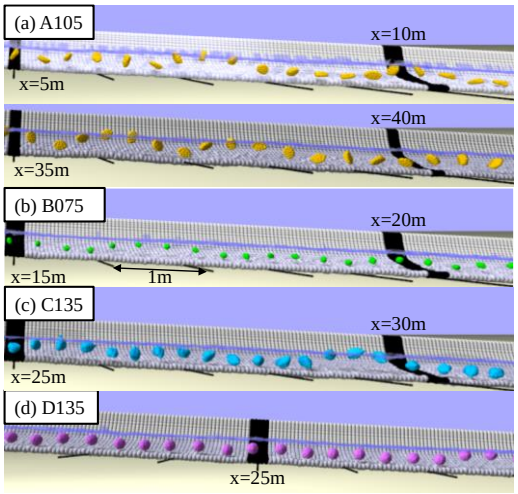

Figure. 3 Trajectories of A105, B075, C135 and D135 every 0.1 second.

3. Results and Discussions

First, characteristics of movement manners of each non-spherical particle are examined. As shown in Fig. 3(a), A105 moves in saltation with the longest or intermediate axis as the rotation axis and in rolling and saltation with the shortest axis as the rotation axis. Massive typed particles (B075 and C135) basically move by rolling or saltation with the longest axis as the rotation axis (Figs. 3(b) and (c)). However, C135, which has a strongly asymmetrical shape, has an unstable rotation, and sometimes leaps greatly after the angular point hits the roughened channel bed. The movement manners of these 3 particles found in the numerical simulations are similar to those of each particle in the Shigemura's experiment. The spherical particle (D135) simply rolls and jumps repeatedly (Fig. 3(d)). Under the conditions of these simulations, each particle is transported in the manner corresponding to its shape regardless of the particle size.

Second, the posture of non-spherical particles is investigated when particles are transported in their characteristic movement manners. Probability density distributions of the projected area of the non-spherical particles in the flow direction are compared (see Fig. 4). When disk typed (A) particles roll or jump with the shortest axis as the rotation axis, probability density distributions are different from the others, but the projected area of the other non-spherical particles in

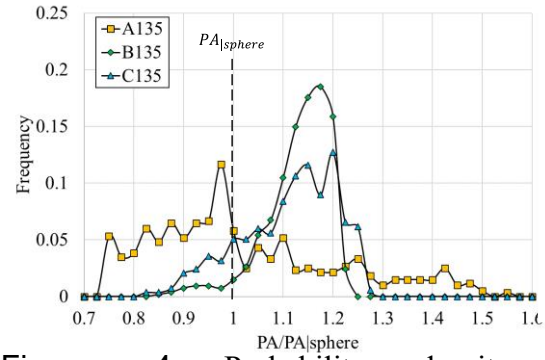

Figure. 4 Probability density distributions of the longitudinal component of the projected area of each non-spherical particle (d = 135 mm).

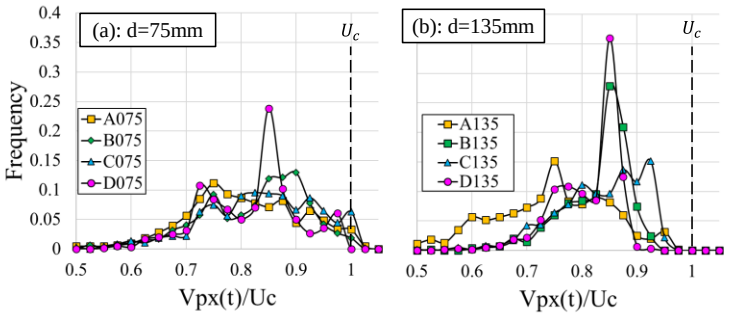

Figure. 5 Probability density distributions of the longitudinal component of the instantaneous particle velocity (Vpx(t)).

Table. 4 Time-averaged particle velocity.

	$\bar{V}_{px}$ [m/s]		
	75mm	105mm	135mm
A: Disk type	3.07	3.13	2.78
B: Massive and symmetric	3.15	3.18	3.16
C: Massive and asymmetric	3.19	3.18	3.18
D: Sphere	3.12	3.22	3.10

The depth averaged velocity (Uc) is 3.88 m/s.

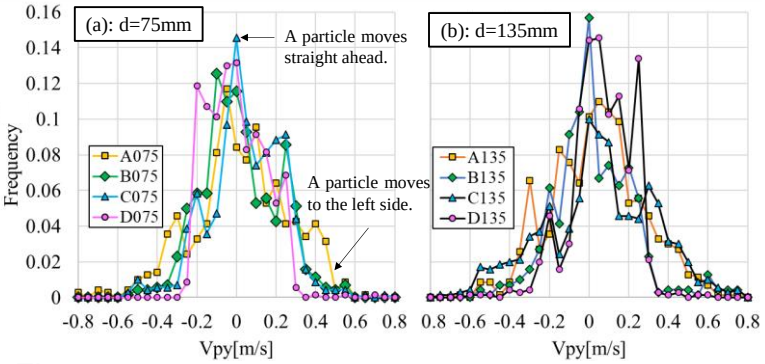

Figure. 6 Probability density distributions of the transverse component of the instantaneous particle velocity (Vpy(t)).

motion are basically larger than that of the sphere with the equivalent volume. This is different from the numerical result of Jain et al. [6] about bedload motions with various shapes over the fixed rough bed. In their numerical simulations, the particle-roughness ratio d/k_s and the Shields number Sh are small about 1.0 and 0.047, respectively, and non-spherical particles roll by interlocking with bed roughness (so called the engagement effect). On the other hand, the particle-roughness ratio and the Shields number in the present simulations are d/k_s (=3.26 ~ 5.87) and Sh (=0.051 ~ 0.092), and the saltation motion is dominant. It is considered that the particle movement postures are affected by these two parameters (d/k_s and Sh) whose values are greatly different in Jain's and our simulations.

Third, effects of particle volume and shape on the particle velocity are investigated. Except for A135, which frequently jumps higher than the water surface, the variation of the longitudinal component of the time-averaged particle velocity ($\bar{V}_{px}$) is very small, at most 4.7 %, as shown in Tab.4. It is also found that there are almost no effect of particle shape on the time-averaged velocity of a particle transported by flows with large Froud number, as shown in the results of previous studies [1] and [2].

In contrast, probability density distributions of the longitudinal component of the instantaneous particle velocity ($V_{px}(t)$) vary greatly depending on the particle volume and shape (see Fig. 5). When the diameter is 75 mm, regardless of the particle shape, the $V_{px}(t)$ is about 0.60 ~ 1.00 times U_c, and shapes of probability density distributions are almost similar. This is because the ratio of the particle diameter to bed roughness d/k_s(= 3.26) is relatively small, and particles that collide head-on with unevenness of the bed increase in number. However, as the particle diameter increases, probability density distributions of the $V_{px}(t)$ clearly differ depending on the particle shape. When the particle shape deviates from the sphere, the peak value of the distribution and the width are small and large, respectively.

Focused on the transverse component of the instantaneous particle velocity $V_{py}(t)$ (see Fig. 6), the $V_{py}(t)$ of spherical particle is at most about ± 0.4 m/s (10 % of U_c), while that of non-spherical particles is at most about ± 0.8 m/s (20 % of U_c), regardless of the particle size. Non-spherical

particles move more three-dimensionally than spherical particles. These analytical results indicate that the motion of arbitrary shaped particles changes in the Shields number, the ratio d/k_s and the particle shape.

As described above, effects of particle shape on the distribution of the instantaneous particle velocity differ depending on the particle size. This mechanism is discussed on the fluid forces and collision forces acting on a moving particle. Fig. 7 shows the longitudinal component of time-averaged fluid force $\bar{F}_{fx}$ acting on each particle dominant in the accelerated motion. $\bar{F}_{fx}$ acting on non-spherical particles such as A075 and C075 are about 1.5 times larger than $\bar{F}_{fx}$ acting on the spherical particle (D075). As the particle size increases, $\bar{F}_{fx}$ acting on non-spherical particles such as A135, B135 and C135 are about 2.0 times larger than the $\bar{F}_{fx}$ acting on the spherical particle (D135). The larger the particle size and the more the shape deviates from the sphere, the greater fluid force and a particle acceleration.

Fig. 8 shows the longitudinal component of the collision force $|F_{cx}|$ that reduces the longitudinal component of the instantaneous particle velocity. The effect of particle shape on the mean value of $|F_{cx}|$ acting on a small particle (d = 75 mm) is very small, however, that on a large particle (d = 135 mm) differs greatly among shapes. These are two reasons. First, except for A135, the mean value of $|F_{cx}|$ also increases as the shape deviates from the sphere. Second, the large sphere (D135) rolls over the bed roughness more easily, and the collision force of D135 is lower than that of D105.

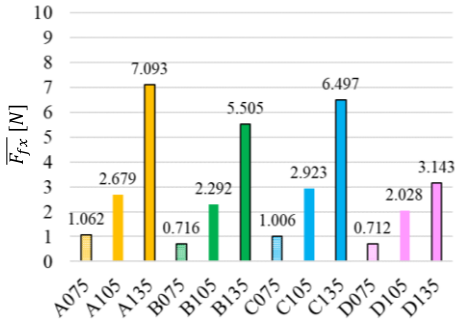

Figure. 7 The longitudinal component of the time-averaged fluid force acting on each particle. Fluid forces are averaged over the time that each particle moves between 7.5 < x < 45 m.

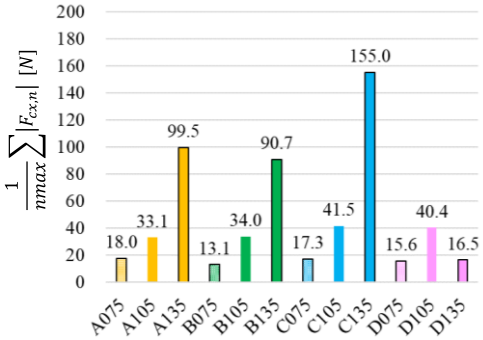

Figure. 8 The longitudinal component of the collision force acting on each particle.

4. Conclusions

Saltation motions of single particles with various volumes and sizes in a turbulent flow over a roughened bed were analyzed to clarify relationships among particle postures, instantaneous velocity, fluid forces and collision forces acting on a particle, and particle volumes and shapes. As the particle diameter increases, effects of the particle shape on its motion become significant. Non-spherical particles are transported with a large projected area in the flow direction and are accelerated by the large fluid force. However, when they hit the channel bed, they generate a large collision force and decelerates. Therefore, the instantaneous velocity of non-spherical particles varies widely. In addition, non-spherical particles have more three-dimensional motion than spherical particles.

These results would contribute to the understanding of fundamental mechanisms in gravel-bed rivers such as the momentum exchange between saltating particles and deposited particles.

Reference

[1] Krumbein (1942). *Eos, Transactions American Geophysical Union, 23(2),* 621-633. https://doi.org/10.1029/TR023i002p00621

[2] Auel et al. (2017). *Earth Surface Processes and Landforms, 42(9),* 1365-1383. https://doi.org/10.1002/esp.4128

[3] Fukuoka, et al. (2014). *Advances in Water Research, 72,*84-96. https://doi.org/10.1016/j.advwatres.2014.05.013

[4] Takakuwa and Fukuoka (2021). *J. JSCE, Ser. B1 (Hydraulic Engineering), 77(2)*, 697-702. https://doi.org/10.2208/jscejhe.77.2_I_697 (*In Japanese*).

[5] Shigemura (2004). *Master of Engineering Thesis, Hiroshima University*. (*In Japanese*).

[6] Jain et al. (2020). *Meccanica, 55*, 299-315. https://doi.org/10.1007/s11012-019-01064-6